The EMBO Journal Vol.18 No.15 pp.4332–4347, 1999

Dbp5, a DEAD-box protein required for mRNA export, is recruited to the cytoplasmic fibrils of nuclear pore complex via a conserved interaction with CAN/Nup159p

Christel Schmitt, Cayetano von Kobbe, Angela Bachi[1], Nelly Panté[2], João P.Rodrigues[3], Cécile Boscheron, Guillaume Rigaut[1], Matthias Wilm[1], Bertrand Séraphin[1], Maria Carmo-Fonseca[3] and Elisa Izaurralde[4]

University of Geneva, Department of Molecular Biology, 30 quai Ernest-Ansermet, CH-1205 Geneva, [2]Institute of Biochemistry, Swiss Federal Institute of Technology (ETH), Universitätstrasse 16, CH-8092 Zürich, Switzerland, [1]European Molecular Biology Laboratory, Meyerhofstrasse 1, D-69117 Heidelberg, Germany and [3]Institute of Histology and Embryology, Faculty of Medicine, University of Lisbon, 1699 Lisboa Codex, Portugal

[4]Corresponding author
e-mail: elisa.izaurralde@molbio.unige.ch

C.Schmitt, C.von Kobbe and A.Bachi contributed equally to this work

Dbp5 is a DEAD-box protein essential for mRNA export from the nucleus in yeast. Here we report the isolation of a cDNA encoding human Dbp5 (hDbp5) which is 46% identical to yDbp5p. Like its yeast homologue, hDbp5 is localized within the cytoplasm and at the nuclear rim. By immunoelectron microscopy, the nuclear envelope-bound fraction of Dbp5 has been localized to the cytoplasmic fibrils of the nuclear pore complex (NPC). Consistent with this localization, we show that both the human and yeast proteins directly interact with an N-terminal region of the nucleoporins CAN/Nup159p. In a conditional yeast strain in which Nup159p is degraded when shifted to the non-permissive temperature, yDbp5p dissociates from the NPC and localizes to the cytoplasm. Thus, Dbp5 is recruited to the NPC via a conserved interaction with CAN/Nup159p. To investigate its function, we generated defective hDbp5 mutants and analysed their effects in RNA export by microinjection in *Xenopus* oocytes. A mutant protein containing a Glu→Gln change in the conserved DEAD-box inhibited the nuclear exit of mRNAs. Together, our data indicate that Dbp5 is a conserved RNA-dependent ATPase which is recruited to the cytoplasmic fibrils of the NPC where it participates in the export of mRNAs out of the nucleus.
Keywords: DEAD-box protein/nuclear pore complex/RNA helicase/RNA nuclear export

Introduction

RNA helicases are enzymes that use energy derived from nucleoside triphosphate hydrolysis to unwind double-stranded RNA (reviewed by Schmid and Linder, 1992; Gorbalenya and Koonin, 1993; Fuller-Pace, 1994; de la Cruz *et al*., 1999). In most cases, the NTPase activity is stimulated by or is dependent on RNA binding, and therefore RNA helicases are considered as RNA-dependent NTPases. Although the precise mechanism by which these enzymes unwind RNA remains to be established, RNA helicases are thought to unwind short duplex regions in RNA molecules in a non-processive manner (Schmid and Linder, 1992; Gorbalenya and Koonin, 1993; Fuller-Pace, 1994). Moreover, RNA helicases may also be implicated in disrupting RNA–protein interactions (Lorsch and Herschlag, 1998a,b; see also Staley and Guthrie, 1999).

Members of the RNA helicase protein family are defined by the presence of seven evolutionarily conserved motifs. The conserved motifs define the helicase core of the protein. Based on the particular consensus sequences of these conserved motifs, RNA helicases have been grouped into two major superfamilies of proteins (SFI and SFII; Gorbalenya and Koonin, 1993). The function of some of the conserved motifs has been elucidated by studying the effects of mutations in ATP and RNA binding, ATP hydrolysis and unwinding activity. Motifs I and II, known as Walker motifs A and B, are defined as the NTPase motifs and are involved in NTP binding and hydrolysis (Walker *et al*., 1982; Rozen *et al*., 1989), while motif VI has been implicated in RNA binding (Pause *et al*., 1993). Depending on the particular consensus sequence in the conserved motif II, SFII RNA helicases are divided further into the DEAD-box and the DExH-box protein families. The prototype of an RNA helicase of the DEAD-box family is the translation initiation factor eIF4A (Linder *et al*., 1989). In the presence of ATP and Mg^{2+}, eIF4A unwinds short RNA duplexes in a non-processive manner (Rogers *et al*., 1999). Processivity is conferred by a second protein, eIF4B, which stimulates the helicase activity of eIF4A allowing the enzyme to unwind longer and more stable RNA duplexes (Rozen *et al*., 1990; Rogers *et al*., 1999).

Comparison of the crystal structure of the hepatitis C virus (HCV) NS3 RNA helicase domain (a SFII DECH-box helicase) with that of bacterial DNA helicases suggests that the folding of the conserved motifs is very similar in both types of enzymes (Subramanya *et al*., 1996; Yao *et al*., 1997; Cho *et al*., 1998; Kim *et al*., 1998; Velankar *et al*., 1999). Due to the high conservation of residues at consensus positions throughout the conserved core, it has been proposed that the structure of the helicase core in other members of the family will closely resemble that of HCV NS3 enzyme. The HCV NS3 helicase consists of three domains arranged in a Y shape (Yao *et al*., 1997; Cho *et al*., 1998; Kim *et al*., 1998). The NTPase motifs I and II are located in domain 1, and define one branch of the Y. Motif VI is located at the opposite branch, in domain 2. Both domains are connected by a flexible hinge that harbours motif III. At the stem of the Y, domain 3 does not contain any conserved motif and is specific to the NS3 enzyme. Domains 1 and 2 undergo large

conformational changes upon binding RNA and the nucleotide cofactor (Yao *et al*., 1997; Cho *et al*., 1998; Kim *et al*., 1998; see also Velankar *et al*., 1999).

Apart from the helicase core, most helicases have variable N- and/or C-terminal unique extensions which have been suggested to play a role in determining substrate specificity and subcellular localization of the enzyme. For instance, the non-conserved N-terminal domain of Prp16p is required for its specific binding to the spliceosome (Wang and Guthrie, 1998). However, specificity cannot be conferred solely by the unique extensions as eIF4A consists essentially of a helicase core without extensions and it is a highly specific enzyme. Therefore, residues exposed at the surface of the helicase core are certainly engaged in the establishment of specific interactions. The observation that, in spite of the functional and structural similarities of their helicase cores, most helicases found in *Saccharomyces cerevisiae* are encoded by essential genes and do not have redundant functions strongly indicates that these enzymes are highly specific (reviewed by de la Cruz *et al*., 1999).

RNA helicases are present in all organisms including prokaryotes, and are likely to participate in all steps of cellular RNA metabolism. In a search for *S.cerevisiae* DEAD-box protein genes using PCR-based strategies, Chang *et al*. (1990) identified five putative RNA helicases. These were called DEAD-box proteins (Dbp) 1–5. Recently, Snay-Hodge *et al*. (1998) and Tseng *et al*. (1998) have shown independently that yeast Dbp5p (yDbp5p) plays an essential role in mRNA export from the nucleus in yeast cells. Furthermore, both groups have reported that Dbp5 is evolutionarily conserved. This conclusion was based on the existence of cDNAs encoding Dbp5 homologues in mouse, *Xenopus laevis*, *Dictyostelium discoideum* and *Schizoaccharomyces pombe*, and on the observation that an antibody raised against yDbp5p recognized a protein of similar size in several species (Snay-Hodge *et al*., 1998; Tseng *et al.*, 1998). yDbp5p is mainly cytoplasmic, but a fraction of the protein associates with nuclear pore complexes (NPCs) (Snay-Hodge *et al*., 1998; Tseng *et al.*, 1998).

Here we report the isolation of a cDNA encoding human Dbp5 (hDbp5). Human Dbp5 is mainly cytoplasmic, but a fraction of the protein associates with the nuclear rim. By immunoelectron microscopy in HeLa and yeast cells and in *Xenopus laevis* oocytes, we have localized a fraction of Dbp5 to the cytoplasmic fibrils of the NPC. Consistent with this localization, we have identified the nucleoporin CAN/Nup159p (von Lindern *et al*., 1992; Kraemer *et al*., 1994, 1995; Gorsch *et al*., 1995) as a directly interacting Dbp5 partner. CAN/Nup159p has been localized to the cytoplasmic fibrils of the NPC (Kraemer *et al*., 1994, 1995; Boer *et al*., 1997) and therefore is a good candidate for mediating the association of Dbp5 with the NPC. Indeed, we show that in a conditional yeast strain in which Nup159p is degraded when shifted to the non-permissive temperature, yDbp5p dissociates from the NPC and localizes entirely to the cytoplasm. Together, these results indicate that Dbp5 is recruited to the NPC via an evolutionarily conserved interaction with CAN/Nup159p. To investigate the functional conservation of hDbp5, we generated a collection of ATPase-deficient mutants. These mutants were tested by microinjection in *X.laevis* oocytes for their ability to inhibit RNA nuclear export in a dominant-negative manner. A mutant protein containing a Glu→Gln change in the conserved DEAD-box exhibits a dominant-negative effect on the nuclear exit of mRNAs. These results indicate that the vertebrate homologue of Dbp5 is also required for the export of mRNAs from the nucleus.

Results

Cloning of the human homologue of Dbp5

To investigate whether the function of Dbp5 in mRNA export has been conserved in higher eukaryotes, we have cloned and characterized its human homologue. Human expressed sequence tags (ESTs) that were likely to represent Dbp5 cDNA clones were identified by database searches. Based on these human ESTs, and on the homology with the murine cDNA, we designed primers to clone the full-length hDbp5 cDNA by RT–PCR. Consideration of the deduced amino acid sequence of the clones obtained by RT–PCR indicates that hDbp5 is 94 and 46% identical to the murine and yeast proteins, respectively (Figure 1A).

To confirm that our cDNA encodes the full-length protein, we compared the migration on SDS–PAGE of the recombinant protein synthesized *in vitro* in rabbit reticulocyte lysates with that of the protein present in HeLa cell extracts. In HeLa cell extracts, hDbp5 was detected by Western blot using rabbit antibodies raised against the bacterially expressed recombinant protein. The *in vitro* translated hDbp5 migrates with the apparent molecular weight of the protein detected in HeLa nuclear or cytoplasmic extracts (Figure 1B). These results, together with the presence of a Kozak consensus sequence surrounding the putative initiation codon and the homology with the murine protein, indicate that the entire open reading frame is likely to be present in our cDNA.

RNA-dependent ATPase and ATP-dependent RNA unwinding activities of human Dbp5

Members of the DEAD-box protein family are predicted to exhibit RNA-dependent NTPase and NTP-dependent RNA-unwindase activities (see Introduction). We have analysed the RNA-binding, ATPase and unwindase activities of recombinant hDbp5 *in vitro* and compared them with those of its yeast homologue. Human and yeast Dbp5 were expressed in *Escherichia coli* as GST fusions. RNA binding was tested by an electrophoretic gel mobility retardation assay. To this end, a ^{32}P-labelled RNA probe was incubated with the recombinant purified proteins, and the resulting complexes were resolved in a native polyacrylamide gel and visualized by autoradiography (Figure 2A). Binding reactions were performed in either the absence or presence of various nucleotides that previously were reported to influence RNA-binding affinity (Lorsch and Herschlag, 1998a,b). These were ATP, AMP-PNP, ATPγS and ADP. In the absence of nucleotides, hDbp5 did not interact with the RNA or the complexes formed were unstable (Figure 2A, lane 2). Inclusion of nucleotides in the binding reactions increased the formation and/or stabilized hDbp5–RNA complexes (Figure 2A, lanes 3–6). It is noteworthy that the complexes obtained in the presence of the nucleotides tested exhibited different mobilities. This is consistent with previous studies showing

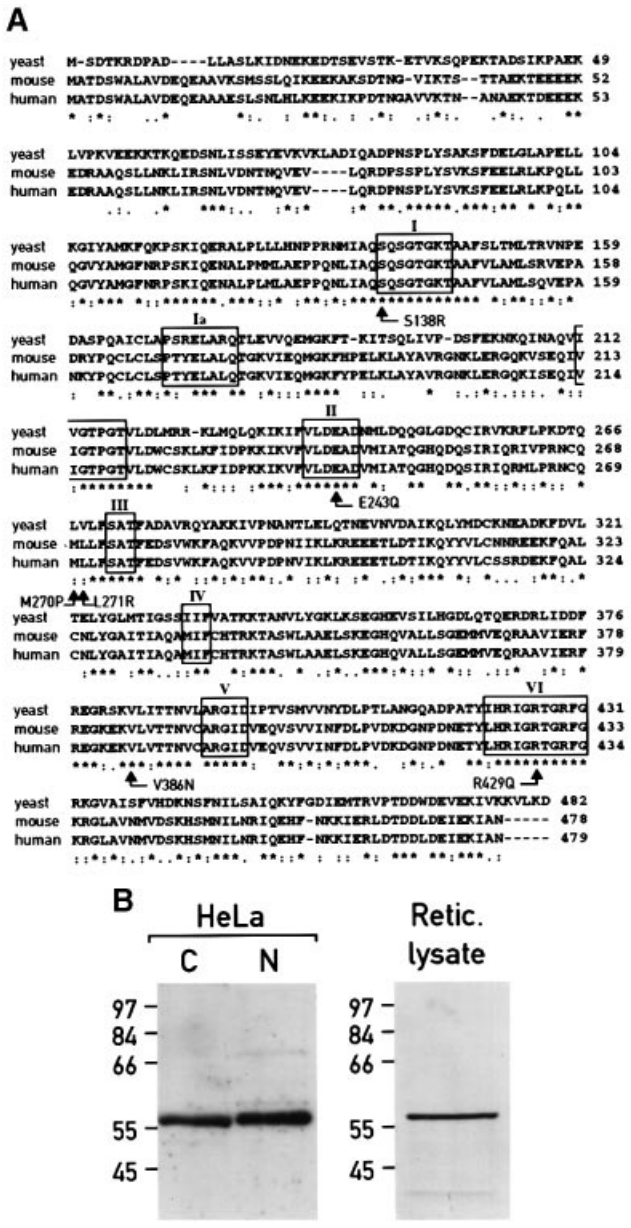

Fig. 1. Cloning of human Dbp5. (**A**) Complete amino acid alignment of predicted Dbp5 protein sequences from human, mouse and yeast using ClustalW1.7. Residue identity between species is highlighted by an asterisk below the sequence. Conserved sequence motifs (denoted by roman numerals) found in the helicase superfamilies are boxed. The positions of the substitution mutants are shown below the primary amino acid sequence of human Dbp5. The sequence data for human Dbp5 have been submitted to DDBJ/EMBL/GenBank under accession No. AJ237946. (**B**) Protein samples from HeLa nuclear (N) and cytoplasmic S-100 (C) extracts were analysed by Western blot using polyclonal anti-hDbp5 antibodies. In parallel, ^{35}S-labelled hDbp5 synthesized *in vitro* in rabbit reticulocyte lysates was analysed.

nucleotide-induced conformational changes in eIF4A (Lorsch and Herschlag, 1998a,b) and in PcrA DNA helicase (Velankar *et al*., 1999). AMP-PNP stabilized the formation of a fast migrating complex (LC: low complex, Figure 2A, lane 4) while ATPγS and ADP stabilized a slow migrating complex (lanes 5 and 6, respectively). The upper complex (UC) corresponds to the major complex obtained with a mutant protein having a Glu→Gln change in the conserved DEAD-box (see Figure 7C). Surprisingly, under the same conditions, GST–yDbp5p did not form stable complexes with the RNA probe (data not shown). This may reflect a difference in affinity and/or in sequence preference between these proteins.

Previously it has been reported that the ATPase activity of recombinant yDbp5p is stimulated by poly(U), poly(A), poly(I), poly(C), poly(G) and tRNA (Tseng *et al.*, 1998). We have compared the ATPase activity of hDbp5 with that of its yeast counterpart *in vitro* in the presence of different polynucleotides (Figure 2B). In the presence of poly(A), poly(U) or poly(C), both proteins hydrolyse >80% of the ATP present in the reaction, in 10 min at 37°C (Figure 2B, lanes 2–4 and 9–11, respectively). Addition of tRNA resulted in ~50% hydrolysis (lanes 6 and 13) while, in the presence of poly(G) or of single-stranded DNA, <40% of the input ATP was hydrolysed. Omission of polynucleotides resulted in ~10% hydrolysis for both proteins (Figure 2B, lanes 8 and 15). This residual activity is likely to be due to the presence of a contaminant activity from *E.coli*. Thus, the RNA-dependent ATPase activity of both hDbp5 and yDbp5p is stimulated most efficiently by poly(A), poly(U) and poly(C), while tRNA, poly(G) and ssDNA are less efficient.

Few members of the DEAD-box protein family have been shown to unwind RNA helices *in vitro* (de la Cruz *et al*., 1999). eIF4A requires a cofactor, eIF4B, in order to unwind RNA duplexes in a processive manner (Rozen *et al*., 1990; Rogers *et al*., 1999). The ATP-dependent helicase activity of yDbp5p was observed when a protein A-tagged version of Dbp5 was expressed in yeast and purified using IgG–Sepharose, suggesting that yDbp5p may require a cofactor to unwind RNA duplexes (Tseng *et al.*, 1998). Similarly, when hDbp5 was immunoprecipitated from HeLa cell S-100 extracts using anti-hDbp5 antibodies coupled to protein A–Sepharose, an unwinding activity was recovered on the beads (Figure 2C, lane 3). The observed RNA-unwinding activity required both ATP (Figure 2C, lane 4) and Mg^{2+} (Figure 2C, lane 5) and was not recovered on beads coated with the pre-immune serum (Figure 2C, lane 6). This activity is probably due to the endogenous hDbp5 protein present in the extracts, as in Western blots the antibodies do not exhibit major cross-reactivities with other proteins (Figure 1B, and data not shown). However, to rule out completely that the observed activity was derived from another unwindase cross-reacting with the antibody, we tested whether recombinant hDbp5 could unwind RNA duplexes upon incubation with HeLa cell S-100 extracts. HeLa cell extracts were incubated with glutathione–agarose beads pre-coated with GST–hDbp5. Upon binding and after extensive washes, beads were tested for the presence of an RNA-unwinding activity. We expected that if hDbp5 requires a cofactor, we should be able to recover this cofactor on the beads. Figure 2D shows that an unwinding activity was recovered on beads pre-coated with GST–hDbp5 (lane 4). No activity was observed when HeLa cell extracts were omitted (lane 3). As a control, three Dbp5 mutants fused to GST were used. Mutants E243Q and E243Q+V386N are ATPase deficient (see below, Figure 7) and therefore cannot unwind the RNA duplex even in the presence of extracts (Figure 2D, lanes 5 and 7). In contrast, mutant R429Q, which exhibits a reduced ATPase activity compared with the wild-type protein

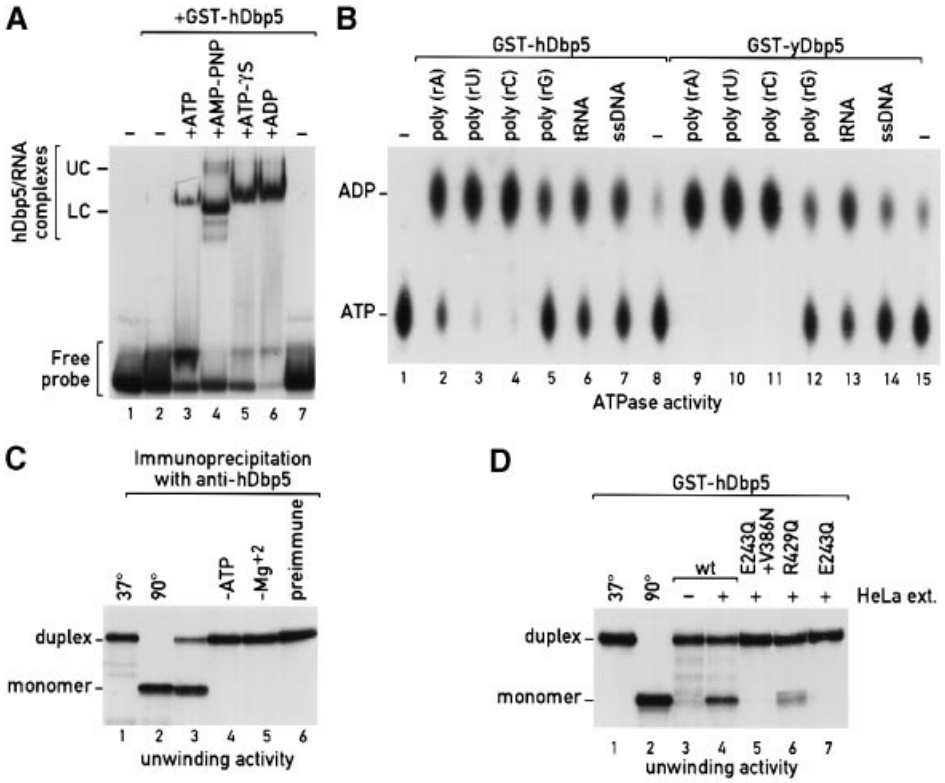

Fig. 2. RNA binding, RNA-dependent ATPase and ATP-dependent unwinding activities of recombinant hDbp5. (**A**) Recombinant hDbp5 binds RNA in a nucleotide-dependent manner. A gel mobility retardation assay was performed with purified recombinant GST–hDbp5. In lanes 3–6, the nucleotides indicated above the lanes were added. The concentration of the nucleotides in the binding reactions was 2 mM, and that of the recombinant protein 0.2 mg/ml. The positions of the free RNA probe (lanes 1 and 7) and of the hDbp5–RNA complexes (lanes 2–6) are indicated on the left. The upper and lower complexes may represent two distinct conformations of hDbp5 bound to the RNA. (**B**) RNA-dependent ATPase activity of purified human and yeast Dbp5 proteins. In lanes 2–7 and 9–14, ATP hydrolysis was stimulated in the presence of the polynucleotides indicated above the lanes. In lanes 8 and 15, no polynucleotide was added. Lane 1 shows the ATP input. The position of ATP and ADP is indicated on the left of the panel. (**C**) hDbp5 immunoprecipitated from HeLa cell S-100 extracts unwinds RNA duplexes *in vitro*. Lane 1, RNA duplex; lane 2, the sample was boiled before loading onto the gel; lane 3, unwinding activity co-immunoprecipitated with anti-hDbp5 polyclonal antibodies; lanes 4 and 5, no unwinding activity was observed when ATP or Mg^{2+} were omitted; lane 6, background activity selected on beads pre-coated with the pre-immune serum. The RNA duplex and the monomer are indicated on the left of the gel. (**D**) Recombinant GST–hDbp5 unwinds RNA duplexes upon incubation with S-100 extracts. HeLa cell extracts were incubated with glutathione–agarose beads pre-coated with GST–hDbp5 (lane 4) or with GST fused to Dbp5 mutants E243Q+V386N (lane 5), R429Q (lane 6) and E243Q (lane 7). Unwinding activity was only observed on beads coated with the wild-type protein (lane 4) and with mutant R429Q. No unwinding activity was observed when the extracts were omitted (lane 3). The bands below the duplex in lane 3 are likely to represent partial degradation of the RNA probe. Symbols are as in (C).

(Figure 7), unwound the RNA duplex upon incubation with the extracts, albeit with a reduced efficiency (Figure 2D, lane 6 versus lane 4). Together, these results suggest that hDbp5 is an ATP-dependent RNA unwindase that requires a cofactor to exhibit unwinding activity. Note that the substrate employed in the assays shown in Figure 2C and D consisted of an RNA duplex of 25 nucleotides ($\Delta G°$ = approximately –44 kcal/mol at 37°C; Turner *et al*., 1988), flanked by 3′-terminal extensions of ~78 nucleotides of single-stranded RNA. Thus, Dbp5 does not require a 5′ single-stranded region on the substrate.

Human Dbp5 is localized in the cytoplasm and at the nuclear rim

Yeast Dbp5p has been localized both to the cytoplasm and to the nuclear envelope (Snay-Hodge *et al*., 1998; Tseng *et al*., 1998; see Figure 5). To investigate the localization of hDbp5, we generated fusion proteins by tagging hDbp5 with the green fluorescent protein (GFP) at its N- or C-terminus. hDbp5–GFP fusions could be vizualized directly upon transfection. Figure 3A–C shows the results obtained when GFP was fused to the N-terminus of hDbp5. In transfected HeLa cells, the majority of the GFP-tagged protein was detected in the cytoplasm, while the nucleoplasm was largely free from staining. Moreover, a fraction of the protein appeared to be concentrated around the nucleus. A similar subcellular localization of hDbp5 was found when the GFP tag was fused to its C-terminus (Figure 3D). The nuclear rim staining became more apparent when cells were treated with digitonin prior to fixation (Figure 3D). The nuclear rim-associated fraction of Dbp5 co-localizes with the labelling produced by monoclonal antibody 414 directed against nucleoporins (Figure 3E and F). Thus, hDbp5, like its yeast homologue, is predominantly cytoplasmic, but a fraction localizes to the nuclear rim.

Identification of an evolutionarily conserved interaction between Dbp5 and CAN/Nup159p

The nuclear rim association of Dbp5 in both HeLa and yeast cells suggests that a fraction of the protein interacts with components of the NPC. Furthermore, experiments shown in Figure 2D suggest that Dbp5 requires a cofactor in order to unwind RNA duplexes. To identify Dbp5

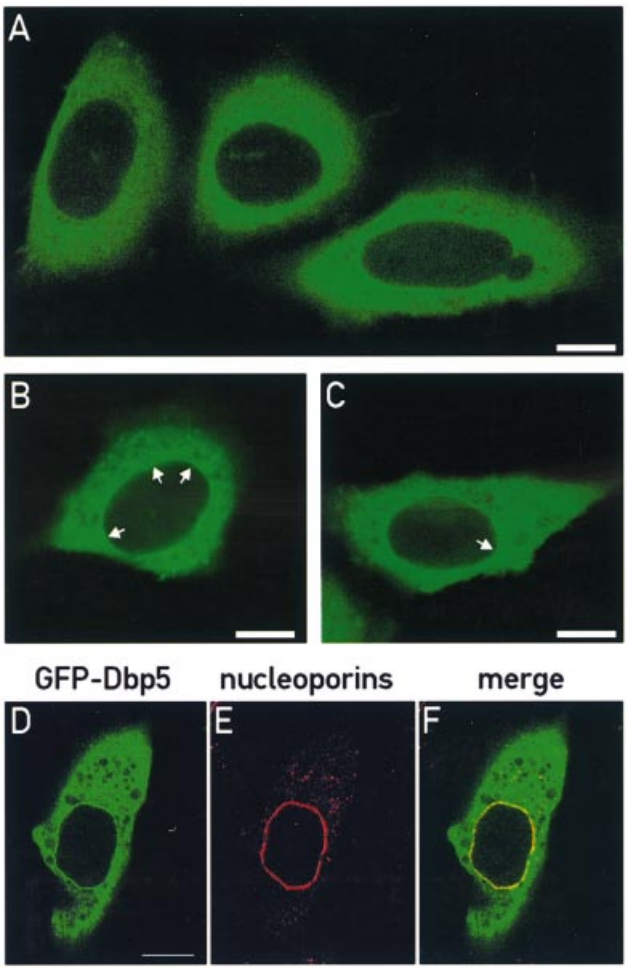

Fig. 3. Human Dbp5 is localized in the cytoplasm and nuclear rim. (**A**–**C**) HeLa cells were transfected with pEGFP-C1 hDbp5 using the calcium phosphate method. Approximately 20 h after transfection, cells were fixed in formaldehyde and observed directly with the fluorescence microscope. The fusion protein is detected predominantly in the cytoplasm. Arrows point to a rim staining at the nuclear periphery. (**D**–**F**) HeLa cells transfected with pEFGP-N3 hDbp5 were permeabilized with digitonin for 2 min before fixation in formaldehyde. The cells were then incubated sequentially with an anti-nucleoporin monoclonal antibody (mAb414) and an appropriate secondary antibody conjugated to Texas red. The superimposition of (D) and (E) confirms that GFP–Dbp5 co-localizes with nucleoporins. Bar, 10 μm.

partners, we have used a novel approach, the tandem affinity purification (TAP) strategy, that allows efficient purification of protein complexes from yeast cell extracts (see Materials and methods). Because of the high degree of similarity between human and yeast Dbp5, their similar localization and function (see below), we expected that identification of its interacting proteins in yeast would lead to the identification of Dbp5 partners in vertebrate cells. The TAP tag was fused to the C-terminus of yDbp5 protein by integrating a DNA cassette into the genome of a haploid cell (Puig *et al*., 1998). The TAP tag consists of a calmodulin-binding peptide followed by a TEV protease cleavage site and two IgG-binding units of *Staphylococcus aureus* protein A (ProtA). Because the tagged protein is the only source of the essential yDbp5 function, and the tagged strain did not display a strong growth phenotype, we conclude that the TAP tag did not abolish Dbp5 protein function. Extracts were prepared from the tagged strain, and Dbp5 with its associated proteins was purified following the two-step affinity purification of the TAP method. Figure 4A shows the proteins eluted from the calmodulin affinity resin. Most of the putative interacting proteins were found in sub-stoichiometric amounts. This does not result from overexpression of the Dbp5 protein that is expressed under the control of its natural promoter, but rather suggests that Dbp5 is not a subunit of a stable multimeric complex. Bands obtained in several selections were excised from the gel, the proteins were in-gel digested with trypsin and the tryptic peptides were identified by mass spectrometry. The peptides sequenced unambiguously identify Nup159p as the protein migrating with an apparent mol. wt of 220 kDa (Gorsch *et al*., 1995; Kraemer *et al*., 1995). The sequenced peptides were ALESVGSDTTFK, SLFVAASGSK and LFDVSAK (using the single-letter amino acid code). Two other bands were identified as Hsp76 and Yra1p (Portman *et al*., 1997). The interaction between Yra1p and yDbp5p was not investigated further.

To determine whether the interaction with Nup159p was conserved, HeLa cell S-100 extracts were fractionated on glutathione–agarose beads on which GST–hDbp5 or GST alone was immobilized. Analysis of the pattern of proteins selected on GST–Dbp5 versus GST by SDS–PAGE revealed one striking difference in the region of 220 kDa due to the presence of a protein in the hDbp5 eluates (Figure 4B, lane 2) which is absent from the GST eluates (lane 3). This band was observed consistently in several selections. Because of its size, and the results obtained with yDbp5p, this protein was predicted to be CAN (von Lindern *et al*., 1992; Kraemer *et al*., 1994), the putative homologue of Nup159p (Gorsch *et al*., 1995; Kraemer *et al*., 1995; Belgareh *et al*., 1998, Hurwitz *et al*., 1998). The identity of this protein was confirmed by Western blot using a polyclonal anti-CAN antibody described by Fornerod *et al*. (1995) (data not shown).

Dbp5 interacts directly with an N-terminal region of CAN/Nup159p

To determine the specificity of the interaction between CAN/Nup159p and Dbp5, we first delineated the domains on CAN/Nup159p that interact with Dbp5. [^{35}S]Methionine-labelled fragments from CAN and Nup159p were synthesized *in vitro* in rabbit reticulocyte lysates and assayed for binding to glutathione–agarose beads coated with either GST–hDbp5, GST–yDbp5p or GST alone. Preliminary experiments indicate that the N-terminal domain of CAN (residues 1–1058) and a shorter fragment encompassing residues 1–586, but not its C-terminal domain (residues 1690–2090), interacted with hDbp5 (data not shown). Figure 4C shows that the fragment of CAN encompassing amino acids 1–586 bound to hDbp5- and yDbp5p-coated beads but not to the control beads having GST alone (lanes 3 and 4 versus lane 2). Further analysis indicates that the C-terminal boundary of the Dbp5-binding domain is located between CAN residues 366 and 433, as fragment 1–433 bound to Dbp5 as efficiently as fragment 1–586, while fragment 1–366 no longer interacted with the helicase (data not shown). Similarly, an N-terminal fragment of Nup159p, comprising residues 1–417, but not a C-terminal fragment

(residues 861–1460), interacted with GST–yDbp5p (Figure 4C, lane 4, and data not shown). Interestingly, hDbp5 did not interact with Nup159p (lane 3), while yDbp5p interacts with both CAN and Nup159p (lane 4). These findings may be explained by the observation that the N-terminal fragments of CAN and Nup159p are only 24% identical over 420 amino acids.

To exclude the possibility that the interactions described above were mediated by an additional factor present in the reticulocyte lysates, we performed GST pull-down assays using recombinant N-terminal fragments of CAN and Nup159 expressed in *E.coli*. Figure 4D shows the results obtained with the N-terminal fragment of Nup159p, residues 1–417, fused to a His_6 tag. This fragment could be selected from *E.coli* lysates on GST–yDbp5p-coated beads (lane 3), but not on beads on which GST–hDbp5 or GST were immobilized (lanes 5 and 7, respectively). These results indicate that the interaction between yDbp5p and Nup159p is direct and is mediated by an N-terminal region of the nucleoporin. This N-terminal domain of Nup159p has been shown previously to contribute substantially to its essential function in mRNA export (Del Priore *et al*., 1997).

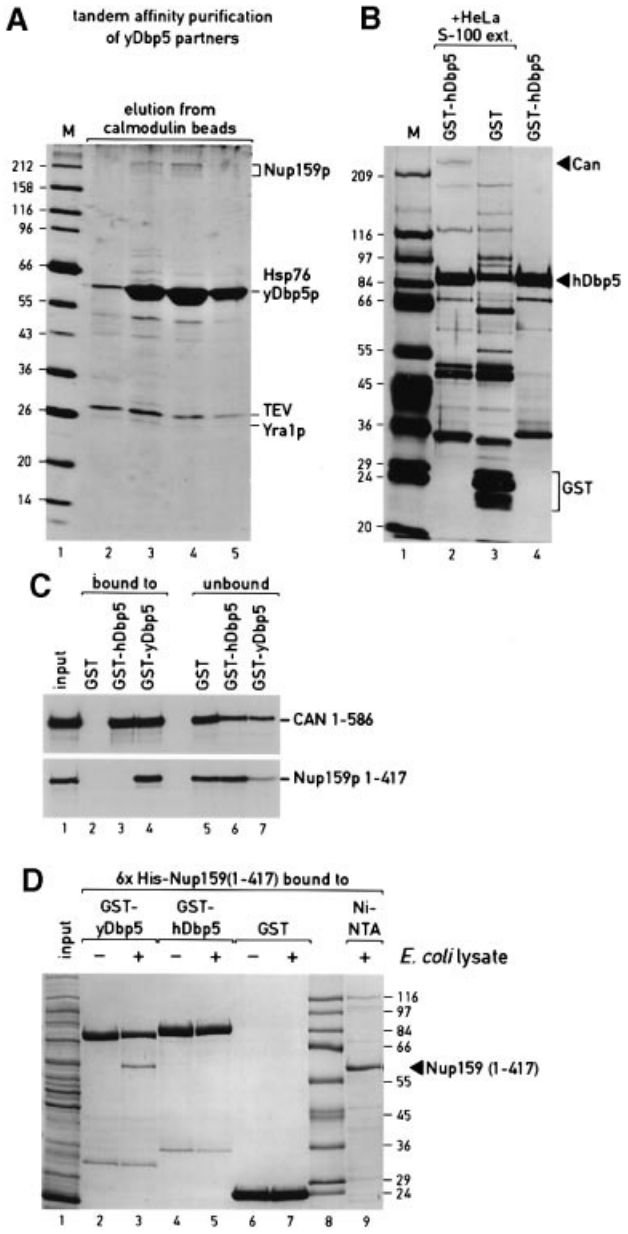

Fig. 4. Identification of CAN/Nup159p as a direct interacting Dbp5 partner. (**A**) Tandem affinity purification of yDbp5p partners. Fractions eluted from the calmodulin affinity resin were analysed on SDS–PAGE followed by silver staining (lanes 2–5). Proteins indicated on the right of the gel were identified by mass spectrometry. (**B**) HeLa cell S-100 extracts were incubated with glutathione–agarose beads on which GST–hDbp5 or GST alone were immobilized (lanes 2 and 3, respectively). After incubation and extensive washes, bound proteins were eluted and analysed by SDS–PAGE followed by silver staining. Lane 4 shows proteins eluted from the GST–hDBP5-coated beads when the extracts were omitted. (**C**) [^{35}S]Methionine-labelled fragments of CAN (residues 1–586) and of Nup159p (residues 1–417) were synthesized *in vitro* in rabbit reticulocyte lysates. Samples of 2 µl from the lysates were incubated with glutathione–agarose beads pre-coated with the recombinant proteins indicated above the lanes. One-tenth of the inputs (lane 1), one-third of the bound fractions (lanes 2–4) and one-twentieth of the unbound fractions (lanes 5–7) were analysed on SDS–PAGE followed by fluorography. (**D**) Lysates from *E.coli* expressing His_6-tagged Nup159p (residues 1–417) were incubated with Ni-NTA beads (lane 9) or glutathione–agarose beads pre-coated with the recombinant proteins indicated above the lanes (lanes 3, 5 and 7). Bound proteins were eluted with SDS sample buffer and analysed on SDS–PAGE followed by Coomassie Blue staining. For each selection, the background obtained in the absence of lysates is shown (lanes 2, 4 and 6). The position of the His-tagged Nup159p N-terminal domain is indicated on the right of the gel.

Nup159p recruits yDbp5p to the NPC

To investigate the role of Nup159p–yDbp5p interaction *in vivo*, we used a yeast strain carrying a conditional *nup159* allele that destabilizes Nup159p at the non-permissive temperature (Nup159Δ1365–1460-ProtA, see also Gorsch *et al*., 1995; Del Priore *et al*., 1997). We expected that if yDbp5p was recruited to the NPC via its interaction with Nup159p, degradation of Nup159p should result in dissociation of yDbp5p from the NPC and its redistribution to the cytoplasm. To visualize its localization directly, the genomic copy of yDbp5p was C-terminally tagged with GFP in a haploid strain. At the permissive temperature, yDbp5p–GFP was detected within the cytoplasm and strongly concentrated around the nucleus (Figure 5). This subcellular location is similar to that reported by Snay-Hodge *et al.* (1998) and Tseng *et al*. (1998). After a 1 h shift to 37°C, yDbp5p–GFP no longer associates with the nuclear envelope and was found in the cytoplasm. Degradation of ProtA-tagged Nup159p was confirmed by Western blot (data not shown). Note that the temperature-sensitive phenotype is lost very rapidly in this strain, suggesting that a spontaneous suppression arises very easily, resulting in a less severe mislocalization of Dbp5. In an isogenic wild-type strain, yDbp5p–GFP was localized at the nuclear envelope at both temperatures (data not shown). Together with the direct interaction between yDbp5p and Nup159p described above, these results indicate that Nup159p provides a docking site for yDbp5p at the NPC.

Dbp5 is located at the cytoplasmic fibrils of the NPC

The experiments described above suggest that Dbp5 is recruited to the NPC via its interaction with CAN/Nup159p. If this were true, Dbp5 must co-localize with the nucleoporin. CAN/Nup159p has been localized to the

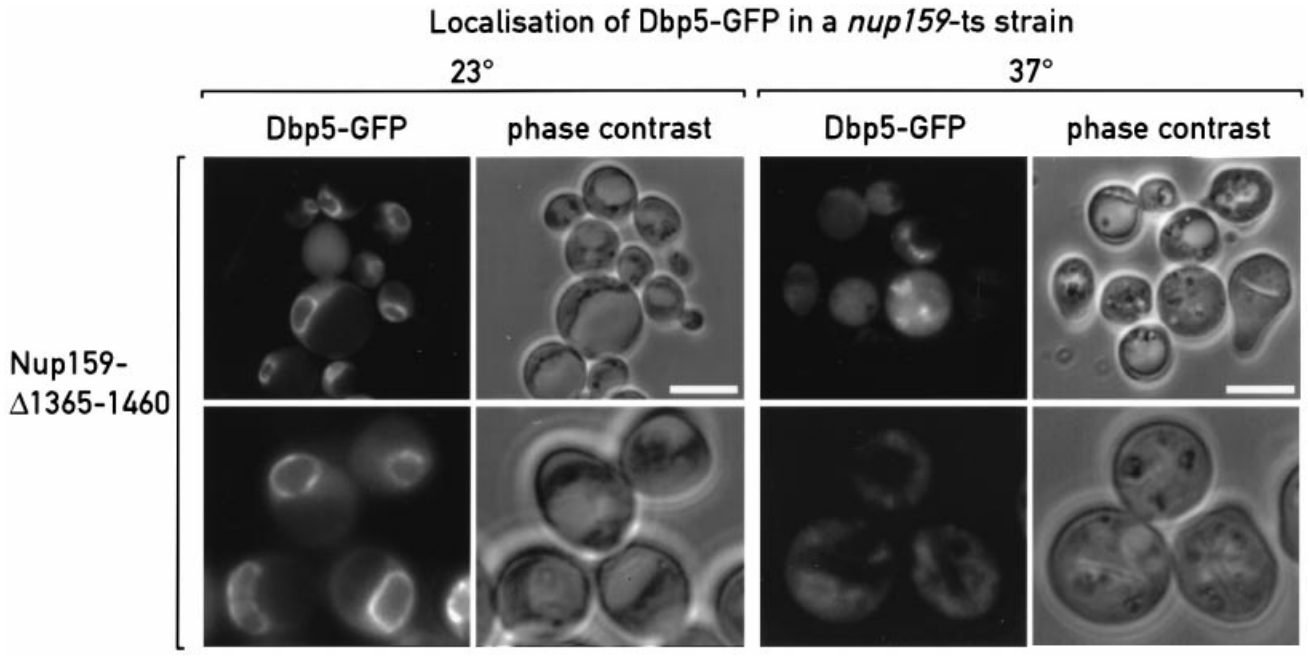

Fig. 5. Localization of GFP-tagged Dbp5 in a yeast strain carrying a conditional *nup159* allele. Yeast cells were grown overnight in liquid YDP at 23°C until mid-exponential phase (OD_{600} of 1). Cells were then either kept at 23°C or shifted for 1 h to 37°C. A 1 ml aliquot of cell suspension was centrifuged briefly and resuspended in 10 µl of water. A 3 µl aliquot of cell suspension was mounted on a microscope slide, sealed with a coverslip and immediately inspected. Nuclear rim staining could be observed readily in cells growing at the permissive temperature. Following incubation at 37°C, the rim staining was no longer observed and Dbp5–GFP localized to the cytoplasm. Scale bar, 10 µm. The lower panels show different fields magnified ~1.5-fold.

cytoplasmic fibrils of the NPC (Kraemer *et al*., 1994, 1995; Boer *et al*., 1997; Hurwitz *et al*., 1998). To determine its location within the NPC, we have visualized yDbp5 following a newly developed protocol which reproducibly yields structurally well-preserved NPCs (Fahrenkrog *et al*., 1998). For this purpose, the yeast strain expressing ProtA-tagged yDbp5p described above was used (TAP-tagged Dbp5). As shown in Figure 6A, we found that in this strain a colloidal gold-conjugated anti-protein A antibody labelled the cytoplasmic periphery of the NPC.

To determine clearly the location of Dbp5 within the NPC at an ultrastructural level, we carried out pre-embedding immunoelectron microscopy on isolated nuclei from *Xenopus* oocytes expressing protein A-tagged hDbp5. As shown in Figure 6B and C, we found that a colloidal gold-conjugated anti-protein A antibody labelled the cytoplasmic periphery of the NPC of oocytes that expressed protein A-tagged hDbp5. The gold particles were detected at a distance of 15–50 nm from the central plane of the NPC, with a mean of 31 nm and an SD of 9 nm (62 gold particles were measured). The distribution of the gold particles from the other symmetry axis of the NPC (i.e. the 8-fold symmetry axis perpendicular to the nuclear envelope) was very broad: gold particles were found within 0 and 50 nm from the 8-fold symmetry axis (with a mean of 15 nm and an SD of 12 nm for $n = 62$). This pattern of labelling is typical of proteins located at or associated with the fibrils that emanate from the cytoplasmic face of the nuclear pore (Yokayama *et al*., 1995; Panté and Aebi, 1996). These fibrils are very flexible and can bend inward into the centre of the nuclear pore, explaining the broad distribution of gold particles associated with the cytoplasmic fibrils. To allow the antibody to reach the nuclear side of the nuclear envelope, some nuclei were treated with Triton X-100 before labelling. As documented in Figure 6D, in this case we also found labelling at the cytoplasmic fibrils of the nuclear pore. However, 20% of the gold particles were located within the nucleus, at distances within 90 and 300 nm from the central plane of the nuclear envelope. In control oocytes, a few gold particles were also detected within the nucleus (data not shown). Thus, we conclude that the nuclear gold particles found in nuclei treated with Triton X-100 probably represent background staining. Note that in yeast cells and in *Xenopus* oocyte nuclei, the cytoplasmic fraction of Dbp5 is not detected, as the soluble cytoplasmic components are removed during sample preparation. Similar results were obtained in HeLa cells; however, in this case, the NPCs were not as well preserved as in yeast and *Xenopus* oocytes (data not shown). Taken together, the results of immunoelectron microscopy in *Xenopus* and yeast nuclei and in HeLa cells demonstrate that the NPC-bound fraction of Dbp5 is located at the cytoplasmic fibrils of the NPC. This localization is in agreement with the previous reported localization of CAN/Nup159p (Kraemer *et al*., 1994, 1995; Boer *et al*., 1997; Hurwitz *et al*., 1998).

Isolation and characterization of defective hDbp5 mutants

To investigate the function of hDbp5 in mRNA nuclear export, we first generated mutants that were expected to be defective in ATP binding and/or hydrolysis and in RNA unwinding activity. Because residues in the conserved motifs are 98% identical to those present in eIF4A, the prototype of the DEAD-box RNA helicase family, we

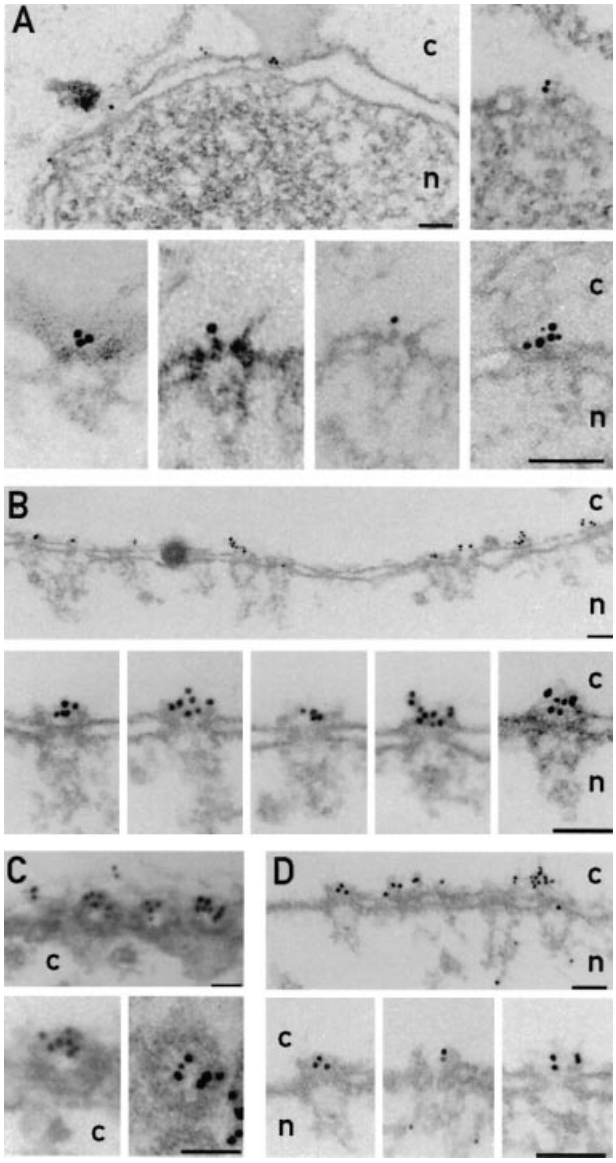

Fig. 6. Dbp5 localizes to the cytoplasmic fibrils of the NPC. (**A**) Localization of Dbp5 in yeast cells expressing protein A-tagged yDbp5p. (**B**–**D**) Tangential and cross-sections of nuclei, and selected examples of gold-labelled nuclear pore tangential and cross-sections from *Xenopus* oocytes after microinjection of an mRNA encoding protein A-tagged hDbp5. Yeast spheroplast or oocyte nuclei were incubated with an anti-protein A antibody conjugated directly to 8 nm diameter colloidal gold particles prior to embedding and thin sectioning. In (D), *Xenopus* oocyte nuclei were permeabilized with Triton X-100 prior to the incubation with the antibody. In all cases, the anti-protein A antibody labelled the cytoplasmic periphery of the nuclear pore with a distribution pattern characteristic of cytoplasmic filament labelling. The cytoplasmic (c) and nuclear (n) side of the nuclear envelope are indicated. Scale bars, 100 nm.

introduced into hDbp5 the equivalent mutations that when present in eIF4A exhibited a dominant-negative effect in translation initiation (Pause *et al.*, 1994). In particular, we have introduced a Ser→Arg change in the conserved motif I (mutant S138R), a Glu→Gln change in the conserved DEAD-box (mutant E243Q) and an Arg→Gln change in motif VI (mutant R429Q) (Figure 1A). We have also combined mutation S138R with E243Q. Finally, we introduced a change of Met270 and Leu271 to Pro and Arg, respectively, and a Val→Asn change at position 386. Similar mutations in yDbp5p conferred a temperature-sensitive phenotype (Snay-Hodge *et al*., 1998).

Mutant proteins were expressed in *E.coli* as GST fusions (Figure 7A, and data not shown). The RNA-dependent ATPase activity of the recombinant proteins was tested *in vitro* in the presence or absence of poly(A). The results are shown in Figure 7B. In the presence of poly(A), the wild-type protein hydrolysed 86% of the ATP present in the reaction in 10 min at 37°C (lane 2). Mutant R429Q exhibited a reduced ATPase activity (63% hydrolysis), while mutant E243Q and the double mutant (E243Q+V386N) failed to hydrolyse ATP in an RNA-dependent manner (Figure 2, lanes 3 and 4 versus lanes 7 and 8).

The RNA-binding activity of the mutant proteins was tested by the electrophoretical retardation assay described in Figure 2A. As for the wild-type protein, the presence of ATP, AMP-PNP, ATPγS and ADP increased the efficiency of RNA binding for all proteins tested. In the absence of nucleotides, mutant E243Q appears to bind RNA more efficiently than the wild-type or other mutant proteins tested (Figure 7C, lane 3 versus lanes 2, 4 and 5). Introduction of mutation V386N in mutant E243Q reduces its RNA-binding activity (lane 4 versus lane 3). Mutant R429Q appeared to form complexes that dissociated during migration. Indeed, although in the presence of nucleotides this mutant bound more efficiently to RNA, the complexes formed dissociated during migration as indicated by the presence of a smear extending from the position of the RNA–protein complexes to that of the free probe. This indicates that this mutant has an impaired RNA binding and provides a rationale for its reduced ATPase activity. Consistent with this is the observation that when the ATPase assays were conducted in the presence of 150 mM KCl, this mutant no longer hydrolysed ATP in an RNA-dependent manner, while the wild-type protein was still active (data not shown). Thus, as is the case for eIF4A, the conserved motif VI is implicated in RNA binding (Pause *et al.*, 1994). Complexes formed with the mutant proteins migrate with mobilities different from those obtained with wild-type Dbp5, suggesting that the mutations may introduce conformational changes in the protein, or may stabilize one particular conformation.

Finally, we tested the different mutants for their ability to interact with CAN *in vitro.* Binding reactions were performed at low salt (150 mM NaCl) or at high stringency in the presence of 300 mM NaCl. Mutants E243Q, E243Q+V386N and R429Q interacted with CAN at the wild-type level under both conditions (Figure 7D, lanes 3–6, and data not shown). In contrast, mutants M270P+L271R, M270P+L271R+E243Q and S138R no longer interacted with CAN (Figure 7E, lanes 4–6, respectively). Surprisingly, addition of mutation E243Q restored binding of mutant S138R up to 50% relative to the wild-type protein when binding reactions were performed in the presence of 150 mM NaCl (Figure 7E, lane 7). However, in the presence of 300 mM NaCl, this mutant failed to bind to CAN (data not shown). Taking into account these findings and the observation that neither the N- nor the C-terminal half of Dbp5 interacted with CAN (Figure 7D, lanes 7 and 8, respectively), we hypothesized that binding to CAN is likely to be mediated by residues

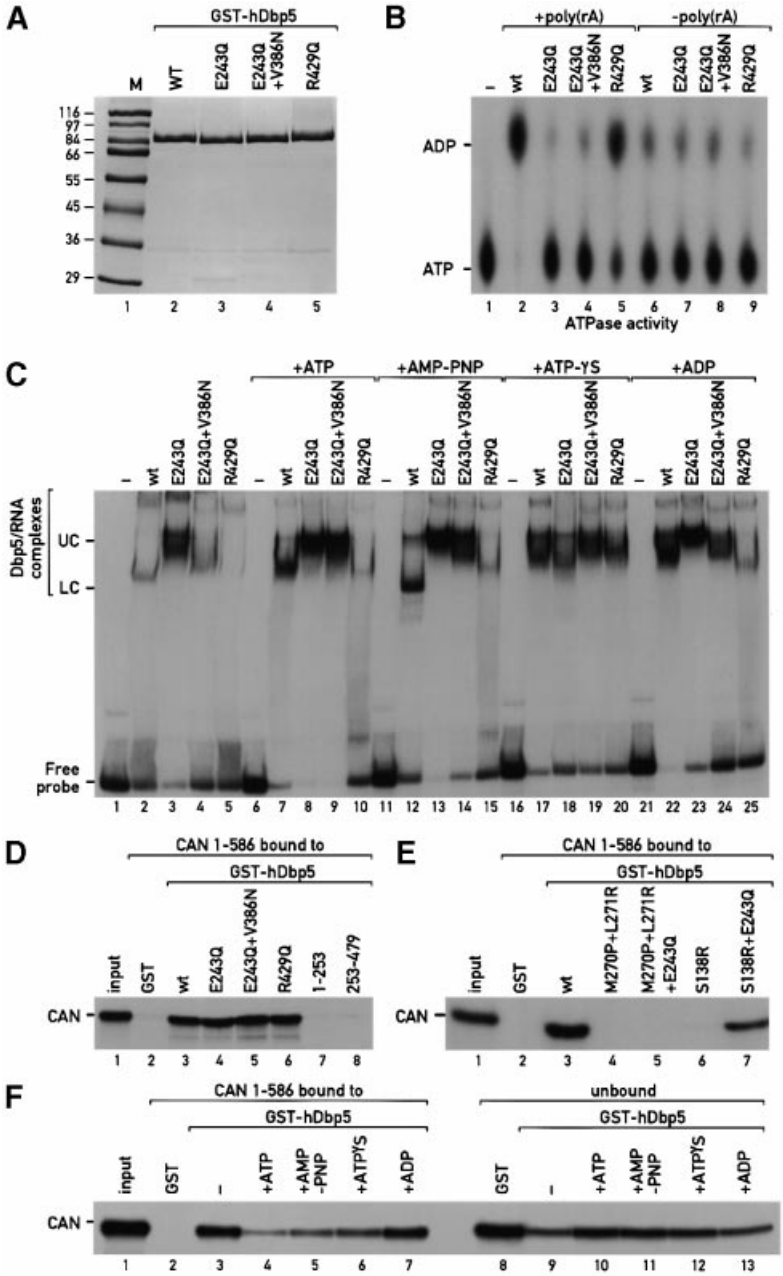

Fig. 7. Characterization of hDbp5 mutants. (**A**) Visualization of the purified wild-type and mutant recombinant hDbp5 proteins by Coomassie staining following SDS–PAGE. (**B**) The ATPase activity of the wild-type and mutant Dbp5 proteins was tested in the presence or absence of poly(A) as indicated above the lanes. Symbols are as in Figure 2B. (**C**) An electrophoretic mobility retardation assay was performed with a labelled RNA probe and the purified recombinant proteins indicated above the lanes. For each protein, binding reactions were performed in the absence of nucleotides (lanes 2–5) or in the presence of ATP (lanes 6–10), AMP-PNP (lanes 11–15), ATPγS (lanes 16–20) or ADP (lanes 21–25). The concentration of the nucleotides in the binding reactions was 2 mM, and that of the recombinant proteins 0.2 mg/ml. The positions of the free RNA probe and of hDbp5–RNA complexes are shown on the left. (**D**–**F**) A [^{35}S]methionine-labelled fragment of CAN (residues 1–586) was synthesized *in vitro* in rabbit reticulocyte lysates. Samples of 2 μl from the lysates were incubated with glutathione–agarose beads pre-coated with the recombinant proteins indicated above the lanes. In (F), binding of CAN to wild-type GST–hDbp5 was analysed in the presence of nucleotide as indicated. One-tenth of the input and one-quarter of the bound fractions were analysed on SDS–PAGE followed by fluorography.

exposed at the surface of the helicase core and is influenced by the overall conformation of the protein. To test this hypothesis, we analysed the interaction between Dbp5 and CAN in the presence of nucleotides which upon binding induce conformational changes in the helicase core. As shown in Figure 7F, the presence of ATP, AMP-PNP and ATPγS reduced the efficiency of CAN binding to Dbp5, while ADP had no effect. This suggest that Dbp5–CAN interaction may be regulated by nucleotide binding and hydrolysis.

Mutants E243Q and E243Q + V386N inhibit the mRNA export pathway

The effect of the mutant proteins in RNA export was examined by microinjection into *Xenopus* oocytes. Purified recombinant proteins (shown in Figure 7A) were injected

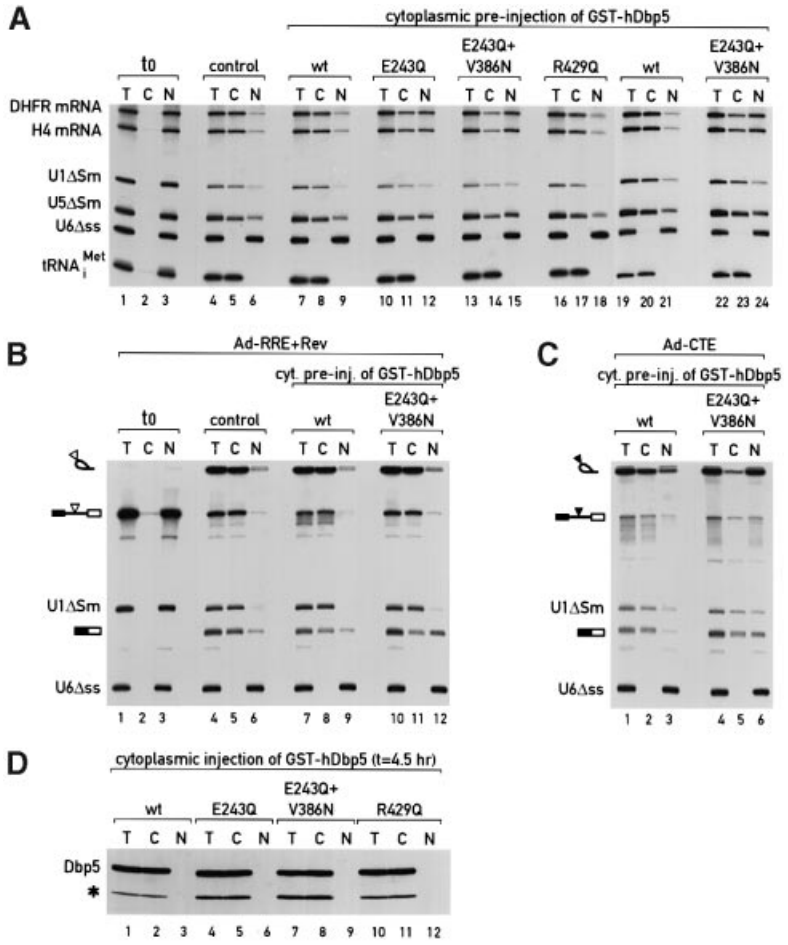

Fig. 8. Inhibition of mRNA export by dominant-negative mutants of hDbp5. (**A**) Purified recombinant GST–hDbp5 and the mutant proteins indicated above the lanes were injected into the oocyte cytoplasm. After 1 h incubation, a second microinjection was performed into the oocyte nuclei with a mixture of radiolabelled RNAs. This mixture consisted of DHFR mRNA, histone H4 mRNA, U1ΔSm, U5ΔSm and U6Δss RNAs, and human initiator methionyl-tRNA. RNA samples from total oocytes (T), cytoplasmic (C) and nuclear (N) fractions were collected 180 min after injection and analysed on 8% acrylamide–7 M urea denaturing gels. One oocyte equivalent of RNA, from a pool of 10 oocytes, was loaded per lane. The concentration of the proteins in the injected samples was ~100 μM. (**B** and **C**) Purified recombinant GST–hDbp5 wild-type or mutant E243Q+V386N were injected into *Xenopus* oocyte cytoplasm 1 h prior to the nuclear injection of a mixture of *in vitro* transcribed ^{32}P-labelled RNAs. This mixture consisted of U1ΔSm RNA, U6Δss RNA and a precursor RNA containing the HIV RRE (Ad-RRE) or the SRV-1 CTE (Ad-CTE) inserted at the intron as indicated. Recombinant HIV Rev protein was co-injected along with samples containing Ad-RRE precursor RNA. The concentration of Rev in the injected samples was 1 μM and that of GST–hDbp5 100 μM. RNA samples from total oocytes (T), cytoplasmic (C) and nuclear (N) fractions were collected 3 h after injection or immediately after injection (t_0: B lanes 1–3) and analysed on 10% acrylamide–7 M urea denaturing gels. One oocyte equivalent of RNA, from a pool of 10 oocytes, was loaded per lane. The mature products and intermediates of the splicing reaction are indicated diagrammatically on the left of the panels. The open and filled triangles represent the RRE and the CTE, respectively. (**D**) Purified recombinant Dbp5 and the mutant proteins indicated above the lanes were injected into *Xenopus* oocyte cytoplasm. Following 4.5 h incubation, protein samples from total oocytes (T), cytoplasmic (C) and nuclear (N) fractions were collected and analysed by Western blot using a rabbit anti-GST antibody. One oocyte equivalent of proteins, from a pool of 10 oocytes, was loaded per lane. The concentration of Dbp5 proteins in the injected samples was ~100 μM. The asterisk indicates a degradation product from the recombinant proteins.

into the oocyte cytoplasm 1 h prior to the nuclear injection of a mixture of labelled RNAs. This mixture consisted of DHFR mRNA, histone H4 mRNA, U1ΔSm, U5ΔSm and U6Δss RNAs, and the human initiator methionyl-tRNA. U6Δss RNA is not exported from the nucleus and lacks protein-binding sites required for nuclear import; it therefore remains at the site of injection and serves as an internal control for nuclear injection and nuclear envelope integrity (Hamm and Mattaj, 1990; Vankan *et al*., 1992). U1ΔSm and U5ΔSm RNAs have a substitution at their Sm-binding site and no longer interact with the Sm proteins; they therefore remain in the cytoplasm after export (Hamm and Mattaj, 1990). Immediately after injection, all RNAs were found in the nuclear fraction (Figure 8A, lanes 1–3). Following a 3 h incubation, in control oocytes, and in oocytes injected with the wild-type protein, ~70% of the DHFR and histone H4 mRNA, 68% of the U1 snRNA and 54% of the U5 snRNA moved to the cytoplasm (Figure 8A, lanes 4–6 and 7–9, respectively). tRNA export was complete (Figure 8A, lanes 4–9). Pre-injection of mutant E243Q inhibited export of mRNAs. Furthermore, when combined with mutation E243Q, mutation V386N increases the inhibitory effect of the mutant protein. Indeed, DHFR and histone H4 mRNA export was reduced to ~40% by mutant E243Q and to 35% by the double mutant. Export of U1 snRNA and U5 snRNA was reduced to ~53 and 40%, respectively, by the double mutant. tRNA export was not affected (Figure 8A, lanes 10–15). Mutant R429Q had no effect when injected at the same concentration (Figure 8A,

lanes 16–18). The inhibitory effect of the double mutant on the export of U snRNAs was no longer observed when the amount of injected protein was decreased by a factor of two (Figure 8A, compare lanes 22–24 with lanes 19–21). In contrast, at this concentration, this mutant inhibited DHFR and histone H4 mRNA export by 58% relative to the export obtained in the presence of the wild-type protein (Figure 8A, lanes 22–24 versus lanes 19–21). The inhibitory effect on mRNA export was obtained reproducibly in several independent experiments using different protein preparations and when the GST tag was changed to two copies of the IgG-binding domain of protein A (data not shown). However, the inhibitory effect on U snRNAs was variable in different experiments (Figure 8B versus C), and was only observed when the mutant proteins were injected at high concentration (Figure 8A).

Prompted by these observations, we also analysed the effect of mutant E243Q+V386N on the export of other RNAs. In particular, we were interested in determining whether this mutant could also inhibit nuclear export driven by the simian type D retrovirus (SRV) constitutive transport element (CTE) which utilizes the mRNA export pathway (Pasquinelli *et al*., 1997; Saavedra *et al*., 1997; Grüter *et al*., 1998). Also, because of the partial inhibitory effect of the double mutant on U snRNA export, we tested its effect on the export driven by the human immunodeficiency virus type 1 (HIV-1) Rev response element (RRE)–Rev system. Rev mediates the export of RRE-bearing RNAs by interacting directly with the export receptor CRM1, which is also involved in the export of U snRNAs (Fornerod *et al*., 1997a). Purified recombinant GST–hDbp5 and mutant E243Q+V386N were injected into *Xenopus* oocyte cytoplasm 1 h prior to the nuclear injection of a mixture of three labelled RNAs. This mixture consisted of U6Δss and U1ΔSm RNAs and an adenovirus-derived precursor mRNA bearing the SRV-1 CTE (Ad-CTE) or the HIV-1 RRE in the intron (Ad-RRE) (Fischer *et al*., 1995; Saavedra *et al.*, 1997). Recombinant HIV Rev protein was included in the injection mixtures containing the Ad-RRE precursor RNA. Immediately after injection, all RNAs were found in the nuclear fraction (Figure 8B, lanes 1–3). Following 3 h of incubation, a substantial amount of the precursor RNA was spliced (Figure 8B, lanes 4–12). About 68% of the resulting mRNA and 85% of the intron-lariat bearing the RRE were found in the cytoplasmic fraction in both control oocytes and oocytes pre-injected with GST–hDbp5 (Figure 8B, lanes 4–9). U1ΔSm RNA export was complete (lanes 4–9). Cytoplasmic pre-injection of mutant E243Q+V386N did not affect splicing efficiency nor the export of the excised intron lariat bearing the HIV RRE (lanes 10–12). In contrast, the export of the spliced mRNA was inhibited and only 40% reached the cytoplasm (lanes 10–12 versus lanes 7–9). In this particular experiment, export of U1 snRNA was not affected (lanes 10–12 versus lanes 7–9). These results suggest that this mutant does not interfere with CRM1-mediated export. On the contrary, Figure 8C shows that pre-injection of mutant E243Q+V386N into the oocyte cytoplasm strongly interferes with CTE-dependent export. Indeed, while ~70% of the excised intron-lariat bearing the CTE was exported in oocytes pre-injected with the wild-type protein, only 18% reached the cytoplasm in the presence of mutant E243Q+V386N (lanes 1–3 versus lanes 4–6). Note that export of the spliced mRNA and of the unspliced pre-mRNA bearing the CTE was also inhibited. These results strongly indicate that mutant E243Q+V386N interferes with CTE-dependent export. Moreover, these findings further demonstrate that the export pathway used by the CTE is shared by the cellular mRNAs and is distinct from that used by the RRE–Rev system (Pasquinelli *et al*., 1997; Saavedra *et al*., 1997; Grüter *et al*., 1998, and references therein). Figure 8D shows that the injected proteins remained cytoplasmic during the time course of the experiment.

In summary, our results indicate that the presence of mutant E243Q or of the double mutant (E243Q+V386N) in the cytoplasmic compartment inhibits the mRNA export pathway in a dominant-negative manner. The inhibitory effect may be explained by the lack of ATPase and unwinding activities of these mutants, as mutant R429Q, which has an impaired ATPase activity, had no effect at the same concentration and, when injected at higher concentrations, partially inhibited mRNA export (data not shown). However, further studies will be required in order to understand the mechanism of inhibition of these mutants.

Discussion

During mRNA nuclear export, dynamic rearrangements of RNA secondary structure and of RNA–protein interactions are likely to occur (reviewed by Daneholt, 1997). Proteins of the DEAD/DExH-box family of RNA-dependent ATPases are thought to play a central role in directing RNA–RNA and RNA–protein rearrangements by unwinding RNA helices and probably disrupting RNA–protein interactions (reviewed by Schmid and Linder, 1992; Gorbalenya and Koonin, 1993; Fuller-Pace, 1994; de la Cruz *et al*., 1999). Recently, a member of this protein family, Dbp5, has been directly implicated in export of mRNAs out of the nucleus in yeast cells (Snay-Hodge *et al*., 1998; Tseng *et al*., 1998). In this report, we show that human Dbp5, like its yeast orthologue, is an RNA-dependent ATPase whose function in mRNA export has been evolutionarily conserved. Furthermore, we show that in both yeast and human cells Dbp5 is recruited to the cytoplasmic fibrils of the NPC via a conserved interaction with the nucleoporin CAN/Nup159p.

In a broad sense, DEAD-box proteins can be considered as ATP-driven switches that produce conformational changes of attached protein domains or associated proteins (Lorsch and Herschlag, 1998a,b). These changes can then be used to rearrange RNA structures or RNA–protein complexes. In this study, we show that hDbp5 exhibits RNA-dependent ATPase activity (Figures 2B and 7B). By using anti-hDbp5 antibodies, or glutathione–agarose beads coated with GST–hDbp5, we could select an RNA-unwinding activity from HeLa cell cytoplasmic extracts (Figure 2C and D). These findings suggest that hDbp5 requires a cofactor to unwind RNA duplexes in a processive manner. However, we have been unable to reconstitute unwinding activity *in vitro* with recombinant Dbp5 in the presence of the N-terminal domain of CAN/Nup159p (data not shown). Therefore, although we cannot

rule out that the full-length CAN/Nup159p is sufficient to activate Dbp5, we favour the hypothesis that an additional cofactor may be implicated.

The demonstration that Dbp5 exhibits RNA-dependent ATPase activity has significant impact on understanding how Dbp5 may function in RNA export. Indeed, conformational rearrangements of large RNPs during the translocation through the NPC may depend on the hydrolysis of ATP by Dbp5. For instance, the ATP hydrolysis-driven conformational changes of Dbp5 may be transduced into movement and/or conformational changes of the emerging mRNP. Alternatively, Dbp5 conformational changes may be transduced into movement and/or conformational changes of the cytoplasmic fibrils of the NPC. Independently of the exact mechanism of action of Dbp5 during export, its direct implication in mRNA nuclear export may account, at least in part, for the energy requirements of this process (Jarmolowski *et al*., 1994).

The terminal step for the RNA export process may occur at the cytoplasmic fibrils of the NPC

In this report, we demonstrate that hDbp5 interacts with an N-terminal region of the nucleoporin CAN while yDbp5 interacts with both CAN and its putative yeast homologue Nup159p. Nup159p is an essential nucleoporin which, like CAN, has already been implicated in mRNA export (Gorsch *et al*., 1995; van Deursen *et al*., 1996; Belgareh *et al*., 1998; Boer *et al*., 1998; Hurwitz *et al*., 1998). The N-terminal domain of Nup159p is not essential for growth, but appears to contribute substantially to its function in mRNA export (Del Priore *et al*., 1997). Indeed, in cells expressing a mutant protein lacking this domain (residues 1–417), nuclear accumulation of polyadenylated RNAs was observed even at the permissive temperature. This defect in mRNA export became more severe following a shift at 37°C. These findings indicate that the N-terminal domain of Nup159p is required for efficient mRNA export (Del Priore *et al*., 1997). Although, currently, it cannot be ruled out that this domain recruits other factors required for export, these observations suggest that recruitment of yDbp5p to the cytoplasmic fibrils of the NPC increases the efficiency of the export process. However, they also indicate that in the absence of the N-terminal domain of Nup159p, yDbp5p can still accomplish its essential function probably due to the high concentration of the protein in the cytoplasm. Alternatively, yDbp5p may interact weakly with other components of the NPC, and these interactions may be temperature sensitive. Indeed, yDbp5p interacts with Gle1p (F.Stutz, personal communication), a nucleoporin showing genetic interaction with Nup159p and yDbp5p (see Snay-Hodge *et al*., 1998).

Aside from interacting directly with Dbp5 (this work), CAN interacts with the mRNA export factor TAP (Katahira *et al*., 1999; our unpublished data) and with the export receptor CRM1 (Fornerod *et al*., 1997b; Neville *et al*., 1997). Binding of CRM1 to CAN requires RanGTP and is stimulated by the export substrate (Askjaer *et al*., 1999). This indicates that the trimeric complex composed of CRM1–RanGTP–NES-substrate would bind CAN immediately after translocation through the NPC. In the cytoplasmic side of the NPC, the RanGAP together with RanBP1 or RanBP2 would promote GTP hydrolysis by Ran and thus the release of the export substrate (Bischoff and Görlich, 1997; Paraskeva *et al*., 1999) and the dissociation of CRM1 from CAN (Askjaer *et al*., 1999; Kehlenbach *et al*., 1999). The close proximity of RanGAP and RanBP2 at the tip of the cytoplasmic fibrils will render this process extremely efficient. Thus, CAN may act as a platform on which the export complexes are dismantled and from which export factors can be returned immediately back to the nucleus. Proteins of the DEAD/DExH-box family of RNA-dependent ATPases are prime candidates to play a role in this disassembling step. If this hypothetical scenario were true, other members of the DEAD/DExH-box family may be implicated in nuclear transport, as Dbp5 appears to be dedicated to the mRNA export pathway (Figure 8). Finally, our data strengthen the hypothesis that CAN is the functional homologue of Nup159p (Kraemer *et al*., 1994, 1995; Gorsch *et al*., 1995; Belgareh *et al*., 1998; Hurvitz *et al*., 1998).

Subcellular localization and functional specificity of Dbp5

Previously, Snay-Hodge *et al*. (1998) and Tseng *et al*. (1998) have shown that a fraction of yDbp5p localizes to the NPC. In this report, we show that both the localization and function of hDbp5 have been evolutionarily conserved. Furthermore, we show that the association of Dbp5 with the NPC is mediated by its direct interaction with CAN/Nup159p (Figures 4, 5 and 6). Although we could map the Dbp5-binding domain from CAN/Nup159p to the N-terminal region of the nucleoporin, the nucleoporin-binding site of Dbp5 could not be reduced to a short sequence. Because mutations in the conserved motifs of the helicase core and the presence of nucleotides alter the interaction between Dbp5 and CAN, we conclude that this interaction may depend on the conformation of the helicase. This suggests that conformational changes on Dbp5 may be transduced to the nucleoporin.

It has been proposed that the unique extensions that most proteins of the DEAD-box family have in addition to their conserved core may determine the subcellular location and the specificity of the enzyme (Wang and Guthrie, 1998). Dbp5 has a unique N-terminal extension; however, this extension is not required for the essential function of the protein as it can be deleted without conferring an obvious phenotype (Snay-Hodge *et al*., 1998). Thus, as is likely to be the case for eIF4A, we conclude that residues exposed at the surface of the helicase core are responsible for determining the specific location and the functional specificity of the enzyme.

Dbp5 is also located within the cytoplasm (Figure 3). The role of the cytoplasmic pool of Dbp5 is unknown. It is possible that recruitment of Dbp5 to the NPC is a dynamic process and Dbp5 dissociates from CAN at one step of the ATP binding and hydrolysis cycle (Figure 7F). The high concentration of Dbp5 in the cytoplasm will ensure a permanent occupancy of its binding sites on the cytoplasmic fibrils. As mentioned above, this appears to be required for efficient mRNA export (Del Priore *et al*., 1997). It is also possible that Dbp5 binds to the exported mRNPs and moves with them to the cytoplasm. However, further studies will be required in order to determine whether the cytoplasmic pool of Dbp5 is associated with mRNPs.

In this study, we show that Dbp5 is involved in the

export of mRNAs but does not play an important role in tRNA export nor in CRM1-mediated export (Figure 8), raising the question of how its functional specificity is determined. In that respect, it is intriguing that Yra1p (Portman *et al*., 1997), an essential hnRNP-like yeast protein, was selected with yDbp5p in our affinity purification (Figure 4A). Similarly, when HeLa cell nuclear extracts were fractionated on GST–hDbp5 affinity columns, we reproducibly have selected hnRNP C1/C2 and hnRNP U (data not shown). Although we cannot rule out that these proteins were tethered on RNA, it is striking that both yeast and human Dbp5 selected an hnRNP protein. Thus it is possible that the substrate specificity of Dbp5 will be determined by its specific interaction with proteins bound to the mRNP. Understanding the mechanism of Dbp5 action in mRNA export and the basis of its functional specificity at the molecular level are important goals for the future.

Materials and methods

Cloning of full-length human hDbp5 cDNA

Full-length human hDbp5 cDNA was obtained by PCR using Expand™ high fidelity enzyme (Boehringer), human HeLa cDNA as a template (Clontech) and primers containing the appropriate restriction sites. Primers were designed based on the human ESTs and on the homology with the murine cDNA. The accession number for the human Dbp5 EST is W27441. PCR fragments were cloned into the *Xho*I–*Eco*RI sites of vectors pGEXCS (Parks *et al*., 1994) and pRSETA (Invitrogen) to generate plasmids pGEXCS-hDbp5 and pRSETA-hDbp5. PCR fragments were also cloned into the *Sph*I–*Bam*HI sites of a derivative of pQE70 vector (Qiagen) having two IgG-binding domains of protein A from *S.aureus* (zz-tag) inserted between the *Eco*RI and *Sph*I sites (pQE70zz-hDBP5-His_6). Dbp5 cDNA was also cloned into the *Nco*I–*Eco*RI sites of a derivative of pBSSK+ vector (Stratagene) having the β-globin 5′-untranslated region inserted between the *Hin*dIII and *Eco*RI sites. Plasmid pBSSK-hDbp5 was used as a template in the *in vitro* coupled transcription–translation system. For expression in HeLa cells, hDbp5 cDNA was cloned as a *Bgl*II–*Eco*RI fragment within the *Bam*HI–*Eco*RI sites of vector pEGFP-C1 (Clontech) and as an *Eco*RI–*Bam*HI fragment into the *Eco*RI–*Bam*HI sites of vector pEGFP-N3 (Clontech).

Cloning of yeast Dbp5p, Nup159p and CAN

Yeast Dbp5p and Nup159p were obtained using Expand™ high fidelity enzyme (Boehringer), with yeast genomic ssDNA as template and primers containing the appropriate restriction sites. Primers were designed based on the yeast genomic DNA (DDBJ/EMBL/GenBank accession Nos U28135 and L40634, respectively). Yeast Dbp5p was cloned into the *Xho*I–*Eco*RI sites of plasmids pGEXCS and pRSETA. A fragment of Nup159p encompassing amino acids 1–417 was cloned into the *Nco*I–*Hin*dIII sites of pRSETB. Plasmid pRSETB-Nup159 1–417 was used as a template in the *in vitro* coupled transcription–translation system. Full-length CAN cDNA (pBS-KS T7-CAN) was kindly provided by Dr Gerard Grosveld. Fragments of CAN encompassing residues 1–586 and 1–1058 were obtained by PCR using plasmid pBS-KS T7-CAN as template. PCR fragments were cloned into the *Nde*I–*Eco*RI sites of pRSETB. pRSETB-CAN plasmids were used as a template in the *in vitro* coupled transcription–translation system. Fragments encompassing CAN residues 1–366 and 1–433 were obtained by linearizing plasmid pRSETB-CAN 1–586 with *Acc*I and *Sca*I, respectively. The linearized plasmids were used as templates in the *in vitro* coupled transcription–translation system.

Mutagenesis and expression of recombinant proteins

All mutations were introduced using an oligonucleotide-directed *in vitro* mutagenesis system from Stratagene (Quick-change site-directed mutagenesis) following the instructions of the manufacturer. Most mutants were generated on pGEXCS-hDbp5 vector and subsequently subcloned into pQE70zz-hDbp5-His_6. Mutations were confirmed by restriction mapping and by sequencing. The sequences of the oligodeoxyribonucleotides are available upon request.

The *E.coli* BL21(DE3) pLysS strain was used when proteins were expressed using the pGEXCS or the pRSET vectors, while *E.coli* M15[pREP4] strain was used for expressing proteins cloned into the pQE vectors. Bacterial pellets were resuspendend in 2× phosphate-buffered saline (PBS), 10% glycerol, 1% Triton X-100, 1 μg/ml aprotinin, 1 μg/ml leupeptin and 1 mM phenylmethylsulfonyl fluoride (PMSF) supplemented with 10 mM imidazole for proteins expressed with a His_6 tag. Lysates were obtained by sonication of bacterial pellets in the appropriate lysis buffer and cleared by centrifugation at 35 000 r.p.m. at 4°C for 90 min in a Beckman Ti60 rotor. Ni-NTA beads superflow (Qiagen) or glutathione–agarose beads (Sigma) were added to bacterial lysates and the mixtures were incubated at 4°C for 1 h. Beads were washed four times with lysis buffer before pouring a column. Columns were washed with three column bed volumes of lysis buffer without Triton X-100 before elution. Proteins bound to glutathione–agarose beads or Ni-NTA beads were eluted with lysis buffer without Triton X-100 supplemented with 20 mM glutathione or 0.5 M imidazole, respectively. The eluted proteins were dialysed against 1.5× PBS containing 5% glycerol. To raise antibodies, hDbp5 was expressed in *E.coli* BL21(DE3) pLysS using the pRSETA-hDbp5 construct. The protein was purified as described above using a denaturing lysis buffer (8 M urea, 0.01 M Tris–HCl pH 8.0, 0.1 M NaH_2PO_4, 10% glycerol, 10 mM imidazole and 1 mM PMSF). The eluted protein was dialysed against PBS containing 10% glycerol and used to raise a rabbit polyclonal antibody. For Western blots, the crude serum was used in a 1:1000 dilution in PBS containing 0.5% Triton X-100 and 5% non-fat milk.

In vitro translation

For generation of ^{35}S-labelled *in vitro* translated proteins, the combined *in vitro* transcription–translation (TnT) kit from Promega was used. Reactions were carried out at 30°C for 2 h. Translation was checked by SDS–PAGE and subsequent fluorography using intensifing solutions from Amersham (Amplify). *In vitro* translated proteins were used directly in binding assays without further purification.

DNA templates for in vitro RNA synthesis

DNA templates for *in vitro* RNA synthesis of Ad-CTE, Ad-RRE, DHFR mRNA, histone H4 mRNA, U5ΔSm, U1ΔSm and U6Δss RNAs, and human methionyl-tRNA have been described previously (Jarmolowski *et al*., 1994; Saavedra *et al*., 1997). Synthesis of Ad-CTE, Ad-RRE, DHFR mRNA, histone H4 mRNA, and U5ΔSm and U1ΔSm RNAs was primed with the m^7GpppG cap dinucleotide, whereas synthesis of U6Δss RNAs was primed with γ-mGTP.

RNA binding assay

For native gel assays, a 77 nucleotide RNA probe was employed. Synthesis and purification of the RNA probe were as previously described (Grüter *et al*., 1998). Homoribopolymers were purchased from Pharmacia and had a mean size of 200 nucleotides. Reactions were carried out in binding buffer: 10 mM HEPES pH 7.9, 50 mM KCl, 5 mM NaCl, 2 mM $MgCl_2$, 0.1 mM EDTA, 10% glycerol, 0.5 mM dithiothreitol (DTT) and 0.025% NP-40. Final sample volumes were 10 μl. A 5 ng aliquot of poly(A) and 0.2 μg of poly(C) and single-stranded herring sperm DNA were used as unlabelled competitors in all binding reactions. The concentration of nucleotides in the binding reaction was 2 mM. Recombinant proteins (2 μg) were added to the reaction mixtures from a diluted stock solution in the same buffer. After 30 min at room temperature, 1 μl of a solution containing 0.05% bromophenol blue in binding buffer was added to the reaction mixtures. Samples were applied to a 5% non-denaturing polyacrylamide gel (19:1 acryl:bisacryl ratio). Electrophoresis was carried out at a constant voltage of 17 V/cm at 4°C in 0.5× TBE buffer and complexes were visualized by autoradiography.

ATPase assay

The ATPase assays were carried out in the presence of 20 mM MES–KOH pH 6.0, 10 mM KOAc, 1% glycerol, 5 mM $MgCl_2$, 1 mM DTT, 0.1 mg/ml poly(A), 1 mg/ml bovine serum albumin (BSA), 1 mM ATP and 0.1 μl of [α-^{32}P]ATP (20 μCi/μl, 3000 Ci/mmol). Reactions (10 μl) were initiated by the addition of 5 μg of purified GST–Dbp5 wild-type or mutant. After incubation for 10 min at 37°C, reactions were stopped by adding 2 μl of proteinase K buffer (50 mM Tris–HCl pH 7.4, 5 mM EDTA, 1.5% SDS, 2 mg/ml proteinase K) and incubated for 20 min at 37°C. Samples of 2 μl were spotted directly onto a PEI–cellulose thin-layer chromatography plate which was developed in 0.6 M potassium phosphate (pH 3.4). In Figure 2B, 1.25 μg of protein was used.

Unwinding assay

The unwinding reactions were carried out on immobilized proteins. A 20 μl aliquot of beads was mixed with 20 μl of helicase buffer (20 mM

HEPES–KOH pH 7.5, 100 mM KCl, 5% glycerol, 5 mM $MgCl_2$ and 1 mM DTT) supplemented with 2 mM ATP, 0.2 mM GTP, 40 U of RNAsin, 5 μg of tRNA and 3500 c.p.m. of ^{32}P-labelled dsRNA substrate. Reactions containing all components were incubated at 37°C for 50 min. Following phenol extraction, 10 μl samples were analysed directly on 12% SDS–PAGE (19:1 acryl:bisacryl ratio).

For the preparation of beads, anti-Dbp5 immune and pre-immune sera were incubated with protein A–Sepharose CL-4B beads (Pharmacia) in 1× PBS and 10% BSA at 4°C for 1 h (1 ml of serum/ml of packed beads). Glutathione–agarose beads coated with GST–Dbp5 were prepared as described for the GST pull-down experiments. About 0.5 μg of recombinant protein was bound per μl of packed beads. In the experiment shown in Figure 2C and D, 200 μl of HeLa S-100 (Dignam *et al*., 1983; protein concentration 7 mg/ml) were incubated at 4°C for 2 h with 20 μl of either protein A–Sepharose beads pre-coated with the immune or pre-immune sera, or 20 μl of glutathione–agarose beads pre-coated with GST–Dbp5 (wild-type or the mutant proteins). Beads were washed five times with 500 μl of 200 mM KCl, 20 mM HEPES–KOH pH 7.5 and 20% glycerol, twice with 500 μl of the same buffer containing 100 mM KCl and 2 mg/ml BSA, and twice with helicase buffer.

Yeast strains cell culture and constructions

The standard protocol for the TAP of Dbp5 and associated partners was used (G.Rigaut and B.Séraphin, unpublished). The experiments described in Figure 5 were carried out in strains isogenic to W303a (*MATa leu2-3,112 his3-11 ade2-1 trp1-1 ura3-1 CAN1-110*). Strains were cultured using rich (YDP, yeast, peptone, dextrose) or defined media (SC, synthetic complete) lacking the appropriate amino acids. The *DPB5* gene was tagged genomically at the 3′ end with the GFP gene (GFP-S65T) using PCR targeting methods described in Wach *et al.* (1997). We have used double modules with GFP as a reporter and *KanMX6* as a selection marker amplified from the plasmid pFA6a-GFP(S65T)-KanMX6. The yeast strain carrying a conditional *nup159* allele was obtained by inserting at the 1365 codon of the *NUP159* gene the TAP tag followed by a stop codon and the *URA3* selectable marker according to the strategy of Puig *et al*. (1998). The strain obtained is temperature sensitive due to instability of the mutant Nup159p at the non-permissive temperature (Gorsch *et al*., 1995; Del Priore *et al*., 1997; and data not shown). The constructed strains were verified either by PCR amplification on DNA from yeast colonies, using primers flanking the sites of integration for GFP-tagged strains, or by Western blotting for protein A-tagged strains. Temperature-sensitive mutants were grown at 23°C (permissive temperature) or shifted to 37°C (restrictive temperature).

GST pull-down assays

Unless indicated otherwise, 5 μg of GST-tagged recombinant proteins immobilized on 20 μl of packed glutathione–agarose beads were used per binding reaction.

For pull-down assays with *in vitro* translated proteins, following binding of GST-tagged recombinant proteins, beads were washed three times with 0.5 ml of IPP buffer (10 mM Tris–HCl pH 8.0, 150 mM NaCl, 5% glycerol) supplemented with 0.1% Triton X-100. Between 2 and 5 μl of *in vitro* synthesized protein in rabbit reticulocyte lysates were used per binding reaction in a final volume of 200 μl of IPP containing 0.1% Triton X-100. Binding was for 1 h at 4°C. Beads were washed four times with 0.5 ml of IPP containing 0.1% Triton X-100. Bound proteins were eluted with SDS sample buffer and analysed by SDS–PAGE followed by fluorography. Alternatively, binding reactions and washes were performed with IPP buffer containing 300 mM NaCl.

When HeLa extracts were used in the pull-down assays (Figure 4B), glutathione–agarose beads were washed twice with 0.5 ml of 0.5 M NaCl, 25 mM HEPES–KOH pH 7.9, and twice with 0.5 ml of binding buffer (100 mM KCl, 20 mM HEPES–KOH pH 7.9, 20% glycerol). HeLa S-100 extracts (1 mg of total protein), prepared as described by Dignam *et al*. (1983), were incubated for 1 h at 4°C with 20 μl of beads in a final volume of 100 μl. The extracts previously were pre-cleared twice on glutathione–agarose beads (100 μl of packed beads/ml of extract). Beads were rotated for 1 h at 4°C, recovered by gentle centrifugation and washed six times with 200 μl of ice-cold binding buffer containing 200 mM KCl. Bound proteins were eluted with 250 mM $MgCl_2$. The eluted proteins were precipitated with 20% trichloroacetic acid (final concentration), resuspended in SDS sample buffer and analysed by SDS–PAGE followed by silver staining.

Protein identification

Proteins eluted from the affinity columns were analysed by SDS–PAGE. Bands of interest were excised and in-gel digested with trypsin (Shevchenko *et al*., 1996). A 0.3 μl aliquot of the total digest solution was analysed by peptide mass mapping on a Bruker REFLEX MALDI time-of-flight mass spectrometer (Bruker-Franzen, Bremen, Germany) using the fast evaporation technique for matrix preparation (Vorm *et al*., 1994). A non-redundant protein database containing >300 000 entries was searched with the peptide masses. In cases when the identification was not certain, the peptide mixture was extracted, desalted on a 100 nl Poros R2 column, eluted directly into a nano-electrospray needle and analysed on a triple quadrupole tandem mass spectrometer (API III, PE-Sciex, Ontario, Canada) (Wilm and Mann, 1996; Wilm *et al*., 1996). Proteins were identified using the sequence tag algorithm and the PeptideSearch program (Mann and Wilm, 1994). Tandem MS experiments were carried on a triple quadrupole mass spectrometer (API III, PE-Sciex, Ontario, Canada).

Immunofluorescence in HeLa cells

HeLa cells were grown as monolayers in minimum essential medium supplemented with 1% non-essential amino acids and 10% fetal calf serum (Gibco-BRL, Gaithersburg, MD). HeLa cells were transfected with either pEGFP-C1 hDbp5 or pEFGP-N3 hDbp5 using the calcium phosphate method. Approximately 20 h after transfection, cells were fixed in formaldehyde and observed directly with the fluorescence microscope. In Figure 3D–F, 20 h after transfection the cells were incubated with 40 μg/ml digitonin in HPEM buffer (65 mM PIPES, 30 mM HEPES, 2 mM $MgCl_2$, 10 mM EGTA, pH 6.9), containing 1 mM PMSF for 2 min on ice. Subsequently the cells were fixed in 3.7% formaldehyde in HPEM for 10 min.

Immunoelectron microscopy in yeast cells and Xenopus oocytes

For immunoelectron microscopy, 8 nm diameter gold particles were prepared and an anti-protein A antibody (Sigma, St Louis, MO) was conjugated directly to the colloidal gold particles as described by Panté *et al*. (1994). Localization of Dbp5 was performed in *Xenopus* and in yeast by pre-embedding labelling. For expression in oocytes, Dbp5 cDNA was cloned into the *Nco*I–*Bam*HI sites of a derivative of pBluescript RN3 kindly provided by Dr V.Doye. This vector contains a zz-tag immediatelly downstream of the β-globin 5′-untranslated region (pRN3zz). Plasmid pRN3zz-hDbp5 was used as a template for the synthesis of an mRNA which was microinjected into the *Xenopus* oocyte cytoplasm. Injected oocytes were incubated at room temperature for 24 h. The nuclei were then dissected manually in low salt buffer (LSB: 1 mM KCl, 0.5 mM $MgCl_2$, 10 mM HEPES, pH 7.5), and cleaned of yolk and other materials by sucking them up and down with a 5 μl pipette in LSB. Freshly isolated nuclei were incubated in the anti-protein A antibody conjugated directly with colloidal gold for 1 h. Next the labelled nuclei were washed three times in LSB and prepared for embedding and thin sectioning exactly as described by Panté *et al.* (1994). For some experiments, isolated nuclei were treated with 0.1% Triton X-100 before labelling. For immunolabelling of yeast, cells expressing yDbp5p tagged with protein A were prepared and pre-embedded labelled according to the method developed by Fahrenkrog *et al*. (1998).

Xenopus laevis oocyte microinjections and RNA analysis

Oocyte injections and analysis of microinjected RNA by denaturing gel electrophoresis and autoradiography analysis were performed as previously described (Jarmolowski *et al.*, 1994; Saavedra *et al.*, 1997). Quantification was performed with a phosphoimager (Bio-Rad). The concentrations of recombinant proteins in the injected samples are indicated in the figure legends.

Acknowledgements

The technical support of Dora Brito, Nathalie Treichel and Emmanuelle Rohrbach is gratefully acknowledged. We wish to thank Drs Nahum Sonenberg for the kind gift of a plasmid pET-hDbp5, Peter Philippsen for plasmid pFA6a-GFP(S65T)-KanMX6G, Kenneth Ryan for plasmid pβglobin-RN3, Valérie Doye for plasmid pβglobin-RN3zz, Lionel Arnaud for plamid pBSSK-βglobin, Dirk Görlich for plamid pQE70zz, and Gerard Grosveld for plasmid pBS-KS T7-CAN and for providing us with anti-CAN antibodies. We are indepted to Lionel Arnaud, Maria Teresa Berciano, Maarten Fornerod, Miguel Lafarga and Patrick Meraldi for their invaluable help. We thank Dr Jeffrey Patton for critical reading of the manuscript, and Nicolas Röggli for the photographic work. This study was supported by the Junta Nacional de Investigação Científica e

Técnologica (Programme PRAXIS XXI) Portugal, the German Ministry of Research and Technology (BMBF), the Swiss National Science Foundation, the State of Geneva and the Human Frontier Science Program Organisation.

References

Askjaer,P. *et al*. (1999) RanGTP-regulated interactions of CRM1 with nucleoporins and a shuttling DEAD-box helicase. *Mol. Cell. Biol*., in press.

Belgareh,N., Snay-Hodge,C., Pasteau,F., Dagher,S., Cole,C. and Doye,V. (1998) Functional characterization of a Nup159p-containing nuclear pore subcomplex. *Mol. Biol. Cell*., **9**, 3475–3492.

Bischoff,F.R. and Görlich,D. (1997) RanBP1 is crucial for the release of RanGTP from importin β-related nuclear transport factors. *FEBS Lett*., **419**, 249–254.

Boer,J.M., Van Deursen,J.M.A., Croes,H.J., Fransen,J.A.M. and Grosveld,G.C. (1997) The nucleoporin CAN/Nup214 binds to both the cytoplasmic and the nucleoplasmic sides of the nuclear pore complex in overexpressing cells. *Exp. Cell Res.*, **232**, 182–185.

Boer,J.M, Bonten-Surtel,J. and Grosveld, G. (1998) Overexpression of the nucleoporin CAN/Nup214 induces growth arrest, nucleocytoplasmic transport defects, and apoptosis. *Mol. Cell. Biol*., **18**, 1236–1247.

Chang,T.-H., Arenas,J. and Abelson,J. (1990) Identification of five putative yeast RNA helicase genes. *Proc. Natl Acad. Sci. USA*, **87**, 1571–1575.

Cho,H.-S., Ha,N.-C., Kang,L.-W., Chung,K.M., Back,S.H., Jang,S.K. and Oh,B.-H. (1998) Crytal structure of RNA helicase from genotype 1b hepatitis C virus. *J. Biol. Chem*., **273**, 15045–15052.

Daneholt,B. (1997) A look at messenger RNP moving through the nuclear pore. *Cell*, **88**, 585–588.

de la Cruz,J., Kressler,D. and Linder,P. (1999) Unwinding RNA in *Saccharomyces cerevisiae*: DEAD-box proteins and related families. *Trends Biochem. Sci.*, **24**, 192–198.

Del Priore,V., Heath,C.V., Snay-Hodge,C.A., MacMillan,A., Gorsch,L.C., Dagher,S. and Cole,C.N. (1997) A structure/function analysis of Rat7p/Nup159p, an essential nucleoporin of *Saccharomyces cerevisiae*. *J.Cell Sci.*, **110**, 2987–2999.

Dignam,J., Lebowitz,R. and Roeder,R. (1983) Accurate transcription initiation by RNA polymerase II in a soluble extract from mammalian nuclei. *Nucleic Acids Res.*, **11**, 1475–1589.

Fahrenkrog,B., Hurt,E., Aebi,U. and Panté,N. (1998) Molecular architecture of the yeast nuclear pore complex: localization of Nsp1p subcomplexes. *J. Cell Biol.*, **143**, 577–588.

Fischer,U., Huber,J., Boelens,W.C., Mattaj,I.W. and Lührmann,R. (1995) The HIV-1 Rev activation domain is a nuclear export signal that accesses an export pathway used by specific cellular RNAs. *Cell*, **82**, 475–483.

Fornerod,M. *et al*. (1995) Relocation of the carboxyterminal part of CAN from the nuclear envelope to the nucleus as a result of leukemia-specific chromosome rearrangements. *Oncogene*, **10**, 1739–1748.

Fornerod,M., Ohno,M., Yoshida,M. and Mattaj,I.W. (1997a) CRM1 is an export receptor for leucine-rich nuclear export signals. *Cell*, **90**, 1051–1060.

Fornerod,M., Vandeursen,J., van Baal,S., Reynolds,A., Davis,D., Gopal Murti,K., Fransen,J. and Grosveld,G. (1997b) The human homologue of yeast Crm1 is in a dynamic subcomplex with CAN/Nup214 and a novel nuclear pore component Nup88. *EMBO J.*, **16**, 807–816.

Fuller-Pace,F.V. (1994) RNAs helicases: modulators of RNA structure. *Trends Cell Biol.*, **4**, 271–274.

Gorbalenya,A.E. and Koonin,E.V. (1994) Helicases: amino acid sequence comparisons and structure–function relationships. *Curr. Opin. Struct. Biol.*, **3**, 419–429.

Gorsch,L.C., Dockendorff,T.C. and Cole,C.N. (1995) A conditional allele of a novel repeat containing yeast nucleoporin Rat7/Nup159 causes both rapid cessation of mRNA export and reversible clustering in nuclear pore complexes. *J. Cell. Biol*., **4**, 939–955.

Grüter,P., Tabernero,C., von Kobbe,C., Schmitt,C., Saavedra,C., Bachi,A., Wilm,M., Felber,B.K. and Izaurralde,E. (1998) TAP, the human homologue of Mex67p, mediates CTE-dependent RNA export from the nucleus. *Mol. Cell*, **1**, 649–659.

Hamm,J. and Mattaj,I.W. (1990) Monomethylated cap structures facilitate RNA export from the nucleus. *Cell*, **63**, 109–118.

Hurwitz,M.E., Strambio-de-Castillia,C. and Blobel,G. (1998) Two yeast nuclear pore complex proteins involved in mRNA export from cytoplasmically oriented subcomplex. *Proc. Natl Acad. Sci. USA*, **95**, 11242–11245.

Jarmolowski,A., Boelens,W., Izaurralde,E. and Mattaj,I.W. (1994) Nuclear export of different classes of RNA is mediated by specific factors. *J. Cell Biol*., **124**, 627–635.

Katahira,J., Strasser,K., Podtelejnikov,A., Mann,M., Jung,J.U. and Hurt,E. (1999) The Mex67p-mediated nuclear mRNA export pathway is conserved from yeast to human. *EMBO J*., **18**, 2593–2609.

Kehlenbach,R.H., Dickmanns,A., Kehlenbach,A., Guan,T. and Gerace,L. (1999) A role for RanBP1 in the release of CRM1 from the nuclear pore complex in a terminal step of nuclear export. *J. Cell Biol*., **145**, 645–657.

Kim,J.L., Morgenstern,K.A., Griffith,J.P., Dwyer,M.D., Thomson,J.A., Murcko,M.A., Lin,C. and Caron,P.R. (1998) Hepatitis C virus NS3 RNA helicase domain with a bound oligonucleotide: the crystal structure provides insights into the mode of unwinding. *Structure*, **6**, 89–100.

Kraemer,D., Wozniak,R.W., Blobel,G. and Radu,A. (1994) The human CAN protein, a putative oncogene product associated with myeloid leukemogenesis, is a nuclear pore complex protein that faces the cytoplasm. *Proc. Natl Acad. Sci. USA*, **91**, 1519–1523.

Kraemer,D.M., Strambio-de-Castillia,C., Blobel,G. and Rout,M.P. (1995) The essential yeast nucleoporin NUP159 is located on the cytoplasmic side of the nuclear pore complex and serves in karyopherin-mediated binding of transport substrate. *J. Biol. Chem.*, **270**, 19017–19021.

Linder,P., Lasko,P.F., Ashburner,M., Leroy,P., Nielsen,P.J., Nishi K. and Slonimski,P. (1989) Birth of the D-E-A-D box. *Nature*, **337**, 121–122.

Lorsch,J.R. and Herschlag,D. (1998a) The DEAD box protein eIF4A. 1. A minimal kinetic and thermodynamic framework reveals coupled binding of RNA and nucleotide. *Biochemistry*, **37**, 2180–2193.

Lorsch,J.R. and Herschlag,D. (1998b) The DEAD box protein eIF4A. 2. A cycle of nucleotide and RNA-dependent conformational changes. *Biochemistry*, **37**, 2194–2206.

Mann,M. and Wilm,M. (1994) Error-tolerant identification of peptides in sequence databases by peptide sequence tags. *Anal. Chem*., **66**, 4390–4399.

Neville,M., Stutz,F., Lee,L., Davis,L.I. and Rosbash,M. (1997) The importin-β family member Crm1p bridges the interaction between Rev and the nuclear pore complex during nuclear export. *Curr. Biol.*, **7**, 767–775.

Panté,N. and Aebi,U. (1996) Import ligand complexes sequentially bind to two distinct nucleopore sites before translocation into the nucleus. *Science*, **273**, 1729–1732.

Panté,N., Bastos,R., McMorrow,I., Burke,B. and Aebi,U. (1994) Interactions and three-dimensional localization of a group of pore complex proteins. *J. Cell Biol*., **126**, 603–617.

Paraskeva,E., Izaurralde,E., Bischoff,F.R., Huber,J., Kutay,U., Hartmann,E., Lührmann,R. and Görlich,D. (1999) CRM1-mediated recycling of snurportin 1 to the cytoplasm. *J. Cell Biol*., **145**, 255–264.

Parks,T.D., Leuther,K.K., Howard,E.D., Johnston,S.A. and Dougherty,W.G. (1994) Release of proteins and peptides from fusion proteins with a recombinant plant virus proteinase. *Anal. Biochem.*, **216**, 413–417.

Pasquinelli,A.E., Ernst,R.K., Lund,E., Grimm,C., Zapp,M.L., Rekosh,D., Hammarskjold,M.-L. and Dahlberg,J.E. (1997) The constitutive transport element (CTE) of Mason–Pfizer monkey virus (MPMV) accesses an RNA export pathway utilized by cellular messenger RNAs. *EMBO J.*, **16**, 7500–7510.

Pause,A., Méthot,N. and Sonenberg,N. (1993) The HRIGRXXR region of the DEAD box RNA helicase eukaryotic initiation factor 4A is required for RNA binding and ATP hydrolysis. *Mol. Cell. Biol*., **13**, 6789–6798.

Pause,A., Méthot,N., Svitkin,Y., Merrick,W.C. and Sonenberg,N. (1994) Dominant negative mutants of mammalian translation initiation factor eIF-4A define a critical role for eIF-4A in cap-dependent and cap-independent initiation of translation. *EMBO J*., **13**, 1205–1215.

Portman,D.S., O'Connor,P. and Dreyfuss,G. (1997) *YRA1*, an essential *Saccharomyces cerevisiae* gene, encodes a novel nuclear protein with RNA annealing activity. *RNA*, **3**, 527–537.

Puig,O., Rutz,B., Luukkonen,B.G., Kandels-Lewis,S., Bragado-Nilsson,E. and Séraphin,B. (1998) New constructs and strategies for efficient PCR-based manipulations in yeast. *Yeast*, **14**, 1139–1146

Rogers,G.W., Richter,N.J. and Merrick,W.C. (1999) Biochemical and kinetic characterization of the RNA helicase activity of eukaryotic initiation factor 4A. *J. Biol. Chem*., **274**, 12236–12244.

Rozen,F., Pelletier,J., Trachel,H. and Sonenberg,N. (1989) A lysine substitution in the ATP binding site of eucaryotic initiation factor 4A abrogates nucleotides binding activity. *Mol. Cell. Biol*., **9**, 4061–4063.

Rozen,F., Edery,I., Meerovitch,K., Dever,T.E., Merrick,W.C. and

Sonenberg,N. (1990) Bidirectional RNA helicase activity of eukaryotic translation initiation factors 4A and 4E. *Mol. Cell. Biol*., **10**, 1134–1144.

Saavedra,C., Felber,B.K. and Izaurralde,E. (1997) The simian retrovirus-1 constitutive transport element (CTE), unlike HIV-1 RRE, utilises factors required for cellular RNA export. *Curr. Biol.*, **7**, 619–628.

Schmid,S.R. and Linder,P. (1992) D-E-A-D protein family of putative RNA helicase. *Mol. Microbiol*., **6**, 283–291.

Shevchenko,A., Wilm,M., Vorm,O. and Mann,M. (1996) Mass spectrometric sequencing of proteins from silver-stained polyacrylamide gels. *Anal. Chem*., **68**, 850–858.

Snay-Hodge,C.A., Colot,H.V., Goldstein,A.L. and Cole,C.N. (1998) Dbp5p/Rat8p is a yeast nuclear pore-associated DEAD-box protein essential for RNA export. *EMBO J*., **17**, 2663–2676.

Staley,J.P. and Guthrie,C. (1999) An RNA switch at the 5′ splice site requires ATP and the DEAD box protein Prp28p. *Mol. Cell*, **3**, 55–64.

Subramanya,H.S., Bird,L.E., Brannigan,J.A. and Wigley,D.B. (1996) Crystal structure of a DExx box helicase. *Nature*, **384**, 379–383.

Turner,D.H., Sugimoto,N. and Freier,S.M. (1988) RNA structure prediction. *Annu. Rev. Biophys. Chem*., **17**, 167–192.

Tseng,S.S.-I., Weaver,P.L., Hitomi,M., Tartakoff,A.M. and Chang,T.-H. (1998) Dbp5p, a cytosolic RNA helicase, is required for poly(A)$^+$ RNA export. *EMBO J*., **17**, 2651–2662.

Van Deursen,J., Boer,J., Kasper,L. and Grosveld,G. (1996) G_2 arrest and impaired nucleocytoplasmic transport in mouse embryos lacking the proto-oncogene *CAN/Nup214*. *EMBO J*., **15**, 5574–5583.

Vankan,P., McGuigan,C. and Mattaj,I.W. (1992) Domains of U4 and U6 snRNAs required for snRNP assembly and splicing complementation in *Xenopus* oocytes. *EMBO J*., **11**, 335–342.

Velankar,S.S., Soultanas,P., Dillinham,M.S., Subramanya,H.S. and Wigley,D.B. (1999) Crystal structure of complexes of PcrA DNA helicase with a DNA substrate indicate an inchworm mechanism. *Cell*, **97**, 75–84.

Von Lindern,M., Fornerod,M., van Baal,S., Jaegle,M., de Wit,T., Bings, A. and Grosveld,G. (1992) The translocation (6;9), associated with a specific subtype of acute myeloid leukemia, results in the fusion of two genes, *dek* and *can*, and the expression of a chimeric, leukemia-specific *dek–can* mRNA. *Mol. Cell. Biol*., **12**, 1687–1697.

Vorm,O., Roepstorff,P. and Mann,M. (1994) Improved resolution and very high sensitivity in MALDI TOF of matrix surfaces made by fast evaporation. *Anal. Chem*., **66**, 3281–3287.

Wach,A., Brachat,A., Alberti-Segui,C., Rebischung,C. and Philippsen,P. (1997) Heterologous HIS3 marker and GFP reporter modules for PCR-targeting in *Saccharomyces cerevisiae*. *Yeast*, **13**, 1065–1075.

Walker,J.E., Saraste,M., Runswick,M.J. and Gay,N.J. (1982) Distantly related sequences in the α- and β-subunits of ATP synthetase, myosin kinases and other enzymes requiring a common nucleotide binding fold. *EMBO J*., **1**, 945–951.

Wang,Y. and Guthrie,C. (1998) PRP16, a DEAH-box RNA helicase, is recruited to the spliceosome primarily via its nonconserved N-terminal domain. *RNA*, **4**, 1216–1229.

Wilm,M. and Mann,M. (1996) Analytical properties of the nano electrospray ion source. *Anal. Chem.*, **66**, 1–8.

Wilm,M., Shevchenko,A., Houthaeve,T., Breit,S., Schweigerer,L., Fotsis,T. and Mann,M. (1996) Femtomole sequencing of proteins from polyacrylamide gels by nano electrospray mass spectrometry. *Nature*, **379**, 466–469.

Yao,N., Hessen,T., Cable,M., Hong,Z., Kwong,A.D., Le,H.V. and Weber,P.C. (1997) Structure of the hepatitis C virus RNA helicase domain. *Nature Struct. Biol*., **4**, 463–467.

Yokoyama,N. *et al*. (1995) RanBP2, a giant nuclear pore protein which binds Ran/TC4. *Nature*, **376**, 184–188.

Received April 20, 1999; revised and accepted June 7, 1999